Electronic Journal of Qualitative Theory of Differential Equations
2025, No. **76**, 1–29; https://doi.org/10.14232/ejqtde.2025.1.76 www.math.u-szeged.hu/ejqtde/

On the integrability and dynamics of the Hide, Skeldon and Acheson differential system

Érika Diz-Pita[1], **Jaume Llibre**[✉2], **M. Victoria Otero-Espinar**[1] and **Claudia Valls**[3]

[1]Departamento de Estatística, Análise Matemática e Optimización, Universidade de Santiago de Compostela, 15782 Santiago de Compostela, Spain
[2]Departament de Matemàtiques, Universitat Autònoma de Barcelona, 08193 Bellaterra, Barcelona, Catalonia, Spain
[3]Departamento de Matemática, Instituto Superior Técnico, Universidade de Lisboa, Lisboa, Portugal

Received 11 October 2024, appeared 23 December 2025
Communicated by Gabriele Villari

Abstract. The family of systems

$$\dot{x} = x(y-1) - \beta z, \quad \dot{y} = \alpha(1-x^2) - \kappa y, \quad \dot{z} = x - \lambda z,$$

where $(x, y, z) \in \mathbb{R}^3$ and α, β, κ, λ are real parameters, was proposed by Hide, Skeldon and Acheson in 1996 for the study of self-excited dynamo action in which a Faraday disc and coil are arranged in series with either a capacitor or a motor. Since then it has been studied by several authors.

Here for the first time we provide, taking into account all values of the parameters, all its 13 types of invariant algebraic surfaces, its 2 polynomial and its 2 rational simple first integrals having at most degree two, and its 6 Darboux invariants coming for the invariant algebraic surfaces of degree two. Moreover, we show how to describe its dynamics in the Poincaré ball when the differential system has either a given first integral, or a given Darboux invariant. Describing the dynamics of the differential system in the Poincaré ball we control the orbits of the system that escape or come from the infinity.

Keywords: Hide–Skeldon–Acheson model, polynomial first integral, rational first integral, invariant algebraic surface, Darboux invariant

2020 Mathematics Subject Classification: 34C05.

1 Introduction and statements of the main results

In this work, we give some results about the integrability and the global dynamics of the Hide–Skeldon–Acheson dynamo model (HSA dynamo model), given by 4-parameter family of systems

$$\dot{x} = x(y-1) - \beta z, \quad \dot{y} = \alpha(1-x^2) - \kappa y, \quad \dot{z} = x - \lambda z, \tag{1.1}$$

✉Corresponding author. Email: jaume.llibre@uab.cat

where $(x, y, z) \in \mathbb{R}^3$ and α, β, κ, λ are real parameters.

The family of systems (1.1) was proposed by Hide, Skeldon and Acheson in 1996 [4] for the study of self-excited dynamo action in which a Faraday disc and coil are arranged in series with either a capacitor or a motor. In this case, $x(t)$ is the current flowing through the dynamo, $y(t)$ is the angular rotation rate of the disc, and $z(t)$ is the angular rotation rate of the motor (or the charge in the capacitor). The parameter α is proportional to the steady applied mechanical couple driving the disc into rotation, β^{-1} measures the moment of inertia of the armature of the motor, and κ and λ are the coefficients of friction in the disc and the motor, respectively.

In [9] the authors study the integrability problem of systems (1.1). They provide some first integrals when the parameter $\alpha \neq 0$. They also prove that for $\alpha, \beta, \kappa \neq 0$ the dynamo model does not admit a polynomial or rational first integral.

In [6] the local and global asymptotical stability of the equilibrium point is discussed. All the orbits of the system are proved to be bounded. The existence of periodic orbits and the Hopf bifurcation is studied, and also the coexistence of three types of attractors: equilibria, hidden periodic attractors and hidden chaotic attractors.

In this paper our goal is to show how invariant algebraic surfaces, first integrals and Darboux invariants help in understanding the global dynamics of polynomial vector fields. Here we do this for the HSA dynamo model. More precisely, the existence of invariant surfaces always simplifies the study of the dynamics of a differential system in $\mathbb{R}^3$ because they separate the phase portrait in invariant pieces by the flow. On the other hand, the existence of a first integral, allows to reduce the study of the dynamics of a differential system in one dimension, and the existence of a Darboux invariant allows to determine the α- and ω-limits of the orbits of the system. In summary, to know one of these three objects helps in understanding the dynamics of a differential system.

One can easily check that systems (1.1) are invariant under the change of variables $(x, y, z) \to (-x, y, -z)$. Consequently if $(x(t), y(t), z(t))$ is a solution to one of the systems (1.1), so is $(-x(t), y(t), -z(t))$ (is symmetric with respect to the y-axis).

Let $\mathbb{R}[x, y, z]$ be the ring of the real polynomials in the variables x, y and z. Let $F = F(x, y, z) \in \mathbb{R}[x, y, z]$. We say that $F = F(x, y, z) = 0$ is an *invariant algebraic surface* of system (1.1) if it satisfies

$$\frac{\partial F}{\partial x}(x(y-1) - \beta z) + \frac{\partial F}{\partial y}(\alpha(1-x^2) - \kappa y) + \frac{\partial F}{\partial z}(x - \lambda z) = KF,$$

where $K = K(x, y, z)$ is a real polynomial of degree at most 1, called the *cofactor* of $F(x, y, z)$. In the next proposition we classify all invariant algebraic surfaces of degree at most two of the HSA dynamo model.

Proposition 1.1. *All the invariant algebraic surfaces of degree one or two that could occur for systems* (1.1) *are given in Table* 1.1 *together with their domains of existence in the parameter space .*

Proposition 1.1 will be proved in Section 3.

Let U be an open and dense subset of $\mathbb{R}^3$. Let $H\colon U \to \mathbb{R}$ a C^1 function non-locally constant. We say that H is a *first integral* of a system (1.1) if H is constant in all the solutions $(x(t), y(t), z(t))$ of that system contained in U. In other words, H must satisfy

$$\frac{\partial H}{\partial x}(x(y-1) - \beta z) + \frac{\partial H}{\partial y}(\alpha(1-x^2) - \kappa y) + \frac{\partial H}{\partial z}(x - \lambda z) = 0,$$

Conditions	$F_k = 0$	**Cofactor**
$\alpha = \beta = \lambda = \kappa = 0$	$F_1 = a - bx + cy - bz + dy^2 + byz$	$K_1 = 0$
$\alpha = \kappa = 0$	$F_2 = a + by + cy^2$	$K_2 = 0$
$\alpha = 0, \beta = \kappa = -\lambda$	$F_3 = a - x - z + yz$	$K_3 = 0$
$\beta = 0$	$F_4 = x$	$K_4 = y - 1$
$\alpha = 0$	$F_5 = y$	$K_5 = -\kappa$
$\alpha = \lambda = 0, \beta = \kappa(1-\kappa),$	$F_6 = -x + ay + (\kappa - 1)z + yz$	$K_6 = -\kappa$
$\alpha = 0, \beta = \kappa(1+\kappa), \lambda = -2\kappa$	$F_7 = -x - (\kappa + 1)z + yz$	$K_7 = \kappa$
$\alpha = 0, \beta = \kappa(1-2\kappa), \lambda = \kappa$	$F_8 = -x + ay^2 + (2\kappa - 1)z + yz$	$K_8 = -2\kappa$
$\alpha = \kappa(1-\kappa) < 0, \beta = 0$	$F_9 = \kappa - 1 - \sqrt{\kappa(\kappa-1)}x + y$	$K_9 = -\kappa - \sqrt{\kappa(\kappa-1)}x$
$\alpha = \kappa(1-\kappa) < 0, \beta = 0$	$F_{10} = \kappa - 1 + \sqrt{\kappa(\kappa-1)}x + y$	$K_{10} = -\kappa + \sqrt{\kappa(\kappa-1)}x$
$\alpha = \kappa(1-\kappa) > 0, \beta = 0$	$F_{11} = (y - (1-\kappa))^2 + \kappa(1-\kappa)x^2$	$K_{11} = -2\kappa$
$\alpha = \kappa(1-\kappa), \lambda = \kappa$	$F_{12} = (y - (1-\kappa))^2 + \kappa(1-\kappa)x^2 + \beta\kappa(1-\kappa)z^2$	$K_{12} = -2\kappa$
$\alpha = 0, \beta = \kappa\lambda - \kappa(1+\kappa)$	$F_{13} = \beta x + \kappa xy - \beta\kappa z$	$K_{13} = y - (1+\kappa)$

Table 1.1: Invariant algebraic surfaces of system (1.1), $F_k = F_k(x, y, z) = 0$, for $1 \leq k \leq 13$. Here $a, b, c, d \in \mathbb{R}$.

on the solutions $(x(t), y(t), z(t))$ of the system (1.1), with fixed $\alpha, \beta, \kappa, \lambda \in \mathbb{R}$, contained in U. A first integral is called *simple* if it is not a function of other first integrals, and the first integral H is called *polynomial* (respectively *rational*) if H is a polynomial (respectively a rational) function. The degree of a polynomial first integral is the *degree* of the polynomial, and the *degree* of a rational function, say $G = P_1/P_2$ being $P_1, P_2 \in \mathbb{R}[x, y, z]$ is the maximum of the degrees of the polynomials P_1 and P_2.

In the next two results we characterize, first all polynomial first integrals of degree at most two of systems (1.1), and second all rational first integrals of degree at most two of systems (1.1).

Proposition 1.2. *All simple polynomial first integrals of degree one or two of systems* (1.1)*, together with the corresponding parameters of existence, are listed in Table* 1.2*.*

The proof of Propositions 1.2 and 1.3 are given in Section 3.

Proposition 1.3. *All simple rational first integrals of degree one or two of systems* (1.1) *that are not polynomial, together with the corresponding parameters of existence, are listed in Table* 1.3*.*

Conditions	**Polynomial first integral**
$\alpha = \kappa = 0$	$H_1 = y$
$\alpha = 0, \beta = \kappa = -\lambda$	$H_2 = x + z - yz$

Table 1.2: Simple polynomial first integrals of systems (1.1), $H_k = H_k(x, y, z)$ for $1 \leq k \leq 2$.

Conditions	Rational first integrals
$\alpha=0,\ \beta=\kappa(1-2\kappa),\ \lambda=\kappa$	$G_1=(-x+(2\kappa-1)z+yz)/y^2$
$\alpha=0,\ \beta=\kappa(1-\kappa),\ \lambda=0$	$G_2=(-x+(\kappa-1)z+yz)/y$

Table 1.3: Simple rational first integrals of systems (1.1), $G_k=G_k(x,y,z)$ for $1\le k\le 2$.

We say that a differential system (1.1) is *completely integrable* if there are two first integrals functionally independent, i.e. the gradients of both first integrals are linear independent except perhaps in a zero Lebesgue measure set.

Corollary 1.4. *If $\alpha=\beta=\kappa=\lambda=0$, the differential system (1.1) is completely integrable with the two first integrals H_1 and H_2 of Table 1.2.*

Corollary 1.4 is given in Section 3. Note that the first integrals H_1 and H_2 are all the rational first integrals of degree one or two, but the systems can have other rational first integrals of higher degree.

An *invariant* of a differential system (1.1) on an open and dense subset U of $\mathbb{R}^3$ is a non-constant C^1 function $I=I(x,y,z,t)$, such that $I(x(t),y(t),z(t),t)$ is constant on all solutions $(x(t),y(t),z(t))$ of that system (1.1) contained in U, i.e.

$$\frac{\partial I}{\partial x}(x(y-1)-\beta z)+\frac{\partial I}{\partial y}(\alpha(1-x^2)-\kappa y)+\frac{\partial I}{\partial z}(x-\lambda z)+\frac{\partial I}{\partial t}=0$$

for all $(x(t),y(t),z(t))\in U$. Note that if an invariant is independent of t it is a first integral.

If the invariant is of the form $I=f(x,y,z)e^{st}$ with f an analytic function in U and $s\in\mathbb{R}\setminus\{0\}$ we say that I is a *Darboux invariant*. A Darboux invariant is *simple* if it is not a function of other Darboux invariants.

Proposition 1.5. *All Darboux invariants $I=f(x,y,z)e^{st}$ with $f(x,y,z)$ formed by the polynomials F_k with $k=1,\dots,13$ of Table 1.1 are given in Table 1.4.*

Conditions	Darboux invariant
$\alpha=0$	$I_1=ye^{\kappa t}$
$\alpha=0,\ \beta=\kappa(1-\kappa),\ \lambda=0$	$I_2=(-x+(\kappa-1)z+yz)e^{\kappa t}$
$\alpha=0,\ \beta=\kappa(1+\kappa),\ \lambda=-2\kappa$	$I_3=(-x-(\kappa+1)z+yz)e^{-\kappa t}$,
$\alpha=0,\ \beta=\kappa(1-2\kappa),\ \lambda=\kappa$	$I_4=(-x+(2\kappa-1)z+yz)e^{2\kappa t}$
$\alpha=\kappa(1-\kappa),\ \beta=0$	$I_5=((y-(1-\kappa))^2+\kappa(1-\kappa)x^2)e^{2\kappa t}$
$\alpha=\kappa(1-\kappa),\ \lambda=\kappa$	$I_6=((y-(1-\kappa))^2+\kappa(1-\kappa)x^2+\beta\kappa(1-\kappa)z^2)e^{2\kappa t}$

Table 1.4: Darboux invariants of systems (1.1), $I_k=I_k(x,y,z)$ for $1\le k\le 6$.

Proposition 1.5 is also proved in Section 3.

Let $\phi_p(t)$ be the solution of a system (1.1) such that $\phi_p(0)=p$, defined on its maximal interval (α_p,ω_p). If $\omega_p=+\infty$, we define the ω-limit set of p as

$$\omega(p)=\Big\{q\in\mathbb{R}^3:\ \exists\{t_n\}\subset\mathbb{R}\text{ with }\lim_{n\to\infty}t_n=\infty\text{ and }\lim_{n\to\infty}\phi_p(t_n)=q\Big\}.$$

In the same way, if $\alpha_p = -\infty$, we define the α-limit set of p as

$$\alpha(p) = \left\{ q \in \mathbb{R}^3 : \exists \{t_n\} \subset \mathbb{R} \text{ with } \lim_{n\to\infty} t_n = -\infty \text{ and } \lim_{n\to\infty} \phi_p(t_n) = q \right\}.$$

While the existence of a first integral allows to reduce in one dimension the study of the dynamics of a differential system in $\mathbb{R}^3$, the existence of a Darboux invariant provides information on the α- and ω-limits of the orbits of the differential system (see Proposition 5 of [8], or Proposition 2.4 in Section 2).

In order to illustrate how to use the existence of a first integral or a Darboux invariant in the study of the global dynamics of the 4-parameter family of systems (1.1) we take the first integral H_2 and the Darboux invariant I_5. This is the content of the next two main results.

Systems (1.1) under the conditions $\alpha = 0$ and $\beta = \kappa = -\lambda$ have the first integral $H_2 = x + z - yz$. In the next theorem we characterize their phase portraits on each level $H_2 = h \in \mathbb{R}$.

Theorem 1.6. *The phase portraits in the Poincaré disc of the differential systems* (1.1) *restricted to the invariant surface* $H_2(x, y, z) = h \in \mathbb{R}$ *under the conditions* $\alpha = 0$ *and* $\beta = \kappa = -\lambda$ *are topologically equivalent to one of the six phase portraits of Figure 1.1. The phase portrait G1 occurs for* $\kappa = 0, h \neq 0$*; G2 for* $\kappa = 0, h = 0$*; G3 for* $\kappa \in (0, 1)$*; G4 for* $k = 1, h \neq 0$*; G5* $\kappa = 1, h = 0$ *and G6 for* $\kappa > 1$ *or* $\kappa = 0$.

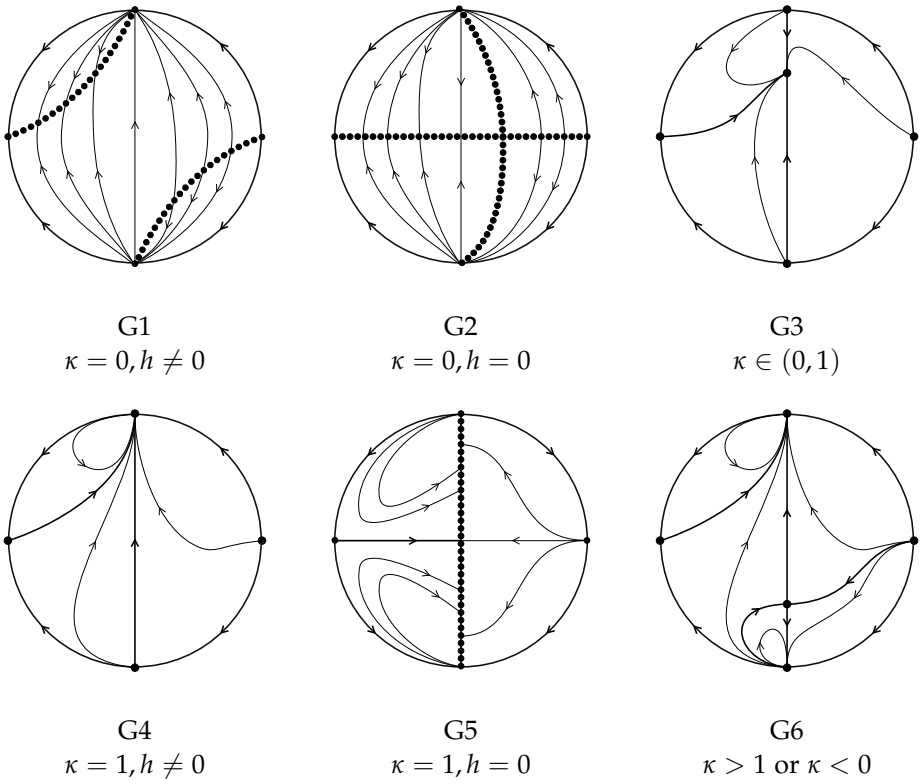

Figure 1.1: Phase portraits of systems (1.1) with $\alpha = 0$ and $\beta = \kappa = -\lambda$ at any level $H_2 = h \in \mathbb{R}$ in the Poincaré disc.

Theorem 1.6 is proved in Section 4.

Systems (1.1) under the conditions $\alpha = \kappa(1 - \kappa) \neq 0$ and $\beta = 0$, have the Darboux invariant $I_5 = ((\kappa - 1 + y)^2 + \kappa(1 - \kappa)x^2)e^{2\kappa t}$. In the next theorem we characterize their dynamics in the Poincaré ball.

We define the infinite equilibrium $S_1 = (\sqrt{\kappa(\kappa-1)}, 0, 0)$ and $S_4 = (-\sqrt{\kappa(\kappa-1)}, 0, 0)$ in the local chart U_1 and $S_3 = (-\sqrt{\kappa(\kappa-1)}, 0, 0)$ and $S_2 = (\sqrt{\kappa(\kappa-1)}, 0, 0)$ in the local chart V_1, and the finite equilibrium $P_1 = (0, 1-\kappa, 0)$.

Theorem 1.7. *The dynamics of the differential systems* (1.1) *under the conditions* $\alpha = \kappa(1-\kappa) \neq 0$ *and* $\beta = 0$ *are described below.*

(a) When $\kappa(\kappa-1) > 0$ *and* $\beta = 0$ *they have two invariant algebraic surfaces* $F_9 = 0$ *and* $F_{10} = 0$ *(see Table 1.1). The boundary of these surfaces are the boundary at infinity of the planes* $y - \sqrt{\kappa(\kappa-1)}x = 0$ *and* $y + \sqrt{\kappa(\kappa-1)}x = 0$*, respectively. Up to topological equivalence there are only two phase portraits on the Poincaré ball for both invariant algebraic surfaces (see Figure 1.2). When* $\kappa(\kappa-1) < 0$ *and* $\beta = 0$ *the invariant surface* $F_{11} = 0$ *corresponds to the straight line* $(0, 1-\kappa, z)$ *with* $z \in \mathbb{R}$*. The boundary of this straight line are the endpoints of the z-axis. The dynamics on this straight line is described by the differential equation* $\dot{z} = -\lambda z$*.*

(b) The phase portraits of systems (1.1) *under the conditions* $\alpha = \kappa(1-\kappa) \neq 0$ *and* $\beta = 0$ *on the infinite sphere is shown in Figures 1.3.*

(b1) When $\kappa(\kappa-1) < 0$ *the boundary at infinity of the plane* $x = 0$ *is filled with equilibria. All the orbits that are not equilibria are heteroclinic orbits starting at an infinite equilibrium with its y-coordinate positive and ending at an infinite equilibrium with its y-coordinate negative.*

(b2) When $\kappa(\kappa-1) > 0$ *the boundary at infinity of the plane* $x = 0$ *is filled with equilibria and there are four additional isolated equilibria* S_k *for* $k = 1, 2, 3, 4$*. On the infinite sphere there are eight separatrices. The equilibria* S_3 *and* S_4 *are the* α*-limit of two separatrices one having its* ω*-limit at the endpoint of the positive z-axis and the other at the endpoint of the negative z-axis. The equilibria* S_1 *and* S_2 *are the* ω*-limits of two separatrices one having its* α*-limit at the endpoint of the positive z-axis and the other at the endpoint of the negative z-axis. The orbits inside the regions delimited by these separatrices and that do not contain equilibria have either* S_4 *as* α*-limit and* S_1 *as* ω*-limit, or* S_3 *as* α*-limit and* S_2 *as* ω*-limit. For all the other orbits: the ones with* $x, y > 0$ *have their* α*-limit at an infinite equilibrium of the plane* $x = 0$ *with* $y > 0$ *and their* ω*-limit at* S_1*; the ones with* $x > 0$*,* $y < 0$ *have their* ω*-limit at one infinite equilibrium of the plane* $x = 0$ *with* $y < 0$ *and their* α*-limit at* S_4*; the ones with* $x < 0$*,* $y > 0$ *have their* α*-limit at one infinite equilibrium of the plane* $x = 0$ *with* $y > 0$ *and their* ω*-limit at* S_2*; the ones with* $x, y < 0$ *have their* ω*-limit at one infinite equilibrium of the plane* $x = 0$ *with* $y < 0$ *and their* α*-limit at* S_3*.*

(c) All the α*- and* ω*-limits for the orbits inside the Poincaré ball, i.e. in* $\mathbb{R}^3$*, are the following:*

(c1) Assume $\kappa(\kappa-1) < 0$*. If* $\lambda > 0$ *all the orbits in* $\mathbb{R}^3$ *have their* ω*-limit at* P_1 *and their* α*-limit at an infinite equilibrium. If* $\lambda < 0$*, with the exception of the equilibria on the straight line* $(0, 1-k, z)$ *with* $z \in \mathbb{R}$*, all the orbits in* $\mathbb{R}^3$ *have their* ω*-limit at the infinite equilibria* $(0, 0, 1)$ *or* $(0, 0, -1)$ *of the Poincaré ball, and their* α*-limit is an infinite equilibrium. If* $\lambda = 0$ *all the orbits in* $\mathbb{R}^3$ *have their* ω*-limit in one of the equilibria of the straight line* $(0, 1-k, z)$ *with* $z \in \mathbb{R}$*, and their* α*-limit is an infinite equilibrium.*

(c2) Assume $\kappa(\kappa-1) > 0$*. For any value of the parameters the* α*-limits of the orbits in* $\mathbb{R}^3$ *are the infinite equilibria* S_3 *and* S_4 *and also the positive and negative endpoints of the z-axis. If* $\lambda = 0$ *and* $\kappa < 0$ *all the equilibria of the straight line* $(0, 1-\kappa, z)$ *with* $z \in \mathbb{R}$ *can be also* α*-limit. If* $\lambda < 0$ *and* $\kappa < 0$*, then the finite equilibrium point* P_1 *can be also an* α*-limit.*

For any values of the parameters the ω-limits are the infinite points S_1 and S_2 and also the positive and negative endpoints of the z-axis. If $\lambda = 0$ and $\kappa > 0$, all the finite equilibria of the straight line $(0, 1-\kappa, z)$ with $z \in \mathbb{R}$ can be also ω-limits. If $\lambda > 0$ and $\kappa > 0$, then the finite equilibrium point P_1 can be also an ω-limit.

Theorem 1.7 is proved in Section 5.

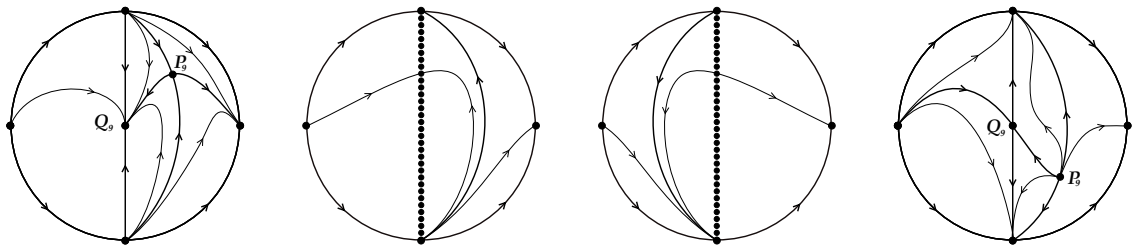

$\lambda > 0$ $\lambda = 0, k > 0$ $\lambda = 0, k < 0$ $\lambda < 0$

Figure 1.2: Phase portraits of systems (1.1) on the invariant surface $F_9 = 0$ and $F_{10} = 0$ with $\alpha = \kappa(1-\kappa) < 0$ and $\beta = 0$.

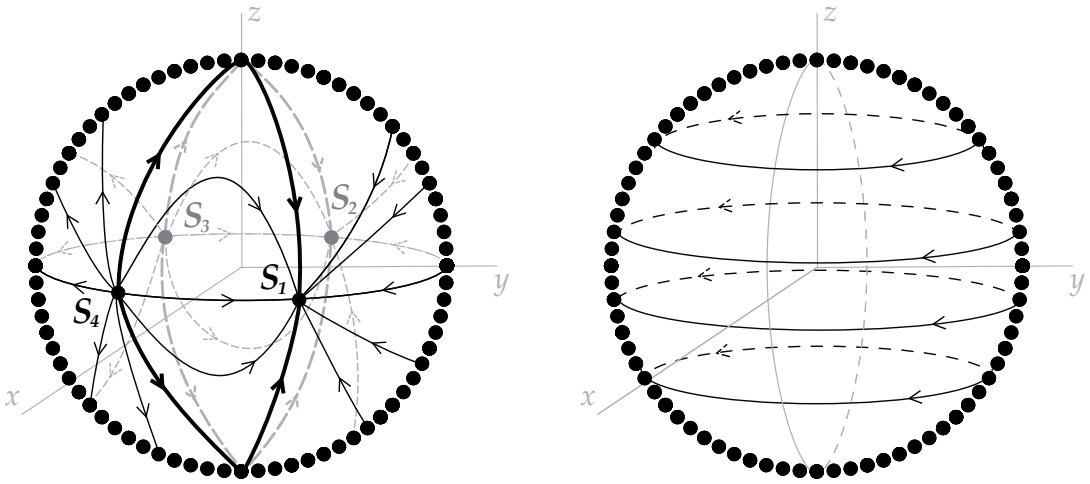

$\kappa(\kappa-1) > 0$ $\kappa(\kappa-1) < 0$

Figure 1.3: Phase portraits of systems (5.1) on the sphere of the infinity.

2 Preliminaries

2.1 Poincaré compactification

2.1.1 Poincaré compactification in dimension 2

Here we introduce the Poincaré compactification, a technique that allows to study the behavior of the orbits of a polynomial differential system near the infinity. This will be used in Sections 4 and 5.

First, we consider the sphere $\mathbb{S}^2 = \{y \in \mathbb{R}^3 : y_1^2 + y_2^2 + y_3^2 = 1\}$, and we call it the *Poincaré sphere*. We identify its tangent plane at the point $(0,0,1)$ with $\mathbb{R}^2$. There, in $\mathbb{R}^2$, we consider a polynomial system of degree d:

$$\dot{x_1} = P_1(x_1, x_2), \quad \dot{x_2} = P_2(x_1, x_2).$$

We get an induced vector field in the northern and southern hemispheres of the sphere with the differential Df^+ and Df^- of the central projections $f^+ : \mathbb{R}^2 \to \mathbb{S}^2$ and $f^- : \mathbb{R}^2 \to \mathbb{S}^2$, defined as $f^{\pm}(x) = \pm(x_1, x_2, 1)/\Delta(x)$, with $\Delta(x) = \sqrt{x_1^2 + x_2^2 + 1}$.

Multiplying the field by y_3^d, we can extend analytically the vector field to the equator, which correspond to the points at infinity of $\mathbb{R}^2$.

This extension is called the *Poincaré compactification* of the original vector field, and the study of this new field near $\mathbb{S}^1$ allows to determine the dynamics of the original field near the infinity.

To make computations we work in the local charts (U_i, ϕ_i) and (V_i, ψ_i) of the sphere $\mathbb{S}^2$, where $U_i = \{y \in \mathbb{S}^2 : y_i > 0\}$, $V_i = \{y \in \mathbb{S}^2 : y_i < 0\}$, $\phi_i : U_i \longrightarrow \mathbb{R}^2$ and $\psi_i : V_i \longrightarrow \mathbb{R}^2$ for $i = 1, 2$ with $\phi_i(y) = \psi_i(y) = (y_m/y_i, y_n/y_i)$ for $m < n$ and $m, n \neq i$.

The expression of the Poincaré compactification in the local chart (U_1, ϕ_1) is

$$(\dot{u}, \dot{v}) = v^d(-uP_1 + P_2, -vP_1), \quad P_i = P_i(1/v, u/v),$$

in the local chart (U_2, ϕ_2) is

$$(\dot{u}, \dot{v}) = v^d(-uP_2 + P_1, -vP_2), \quad P_i = P_i(u/v, 1/v).$$

The expression for the Poincaré compactification in the local charts (V_i, ψ_i), with $i = 1, 2, 3$ is the same as in the local charts (U_i, ϕ_i) multiplied by $(-1)^{d-1}$.

As we want to study the behavior near the infinity, we study the *infinite equilibrium points*, i.e., the equilibrium points of the Poincaré compactification over the equator $\mathbb{S}^1$. If $y \in \mathbb{S}^1$ is an infinite equilibrium point, then $-y$ is also an infinite equilibrium point and they have the same or opposite stability depending on the degree of the system. Then, it is enough to study the infinite equilibrium points in the local chart U_1 and the origin of the local chart U_2.

More information about the Poincaré compactification in dimension 2 can be found in Chapter 5 of [3].

2.1.2 Poincaré compactification in dimension 3

The technique of the Poincaré compactification can be extended to higher dimensions. In particular, we use this technique in dimension 3 in Section 5. As the ideas are the same explained before, we just include here the expressions obtained in the local charts U_1, U_2 and U_3 for a polynomial system in $\mathbb{R}^3$ of degree d

$$\dot{x} = P_1(x, y, z), \quad \dot{y} = P_2(x, y, z), \quad \dot{z} = P_3(x, y, z).$$

More details about the Poincaré compactification in dimension n can be found in [1].

The phase portrait in the local chart U_1 is given by the system

$$(\dot{u}, \dot{v}, \dot{w}) = w^d(-uP_1 + P_2, -vP_1 + P_3, -wP_1), \quad P_i = P_i(1/w, u/w, v/w),$$

where u and v are the coordinates of the tangent plane to the sphere $\mathbb{S}^2$ at the point $(1,0,0)$.

The phase portrait in the local chart U_2 is given by the system

$$(\dot{u},\dot{v},\dot{w}) = w^d(-uP_2 + P_1, -vP_2 + P_3, -wP_2), \quad P_i = P_i(u/w, 1/w, v/w),$$

with the coordinates u, v of the tangent plane to the sphere at $(0,1,0)$.

In the local chart U_3 the phase portrait is given by

$$(\dot{u},\dot{v},\dot{w}) = w^d(-uP_3 + P_1, -vP_3 + P_2, -wP_3), \quad P_i = P_i(u/w, v/w, 1/w),$$

and now u and v are the coordinates of the tangent plane to the sphere $\mathbb{S}^2$ at the point $(0,0,1)$.

The following result is proved in [7].

Lemma 2.1. *Let $f(x,y,z) = 0$ be an algebraic surface of degree m in $\mathbb{R}^3$. The extension of this surface to the boundary of the Poincaré ball is contained in the surface defined by*

$$w^m f\left(\frac{x}{w}, \frac{y}{w}, \frac{z}{w}\right) = 0, \quad w = 0.$$

2.2 Invariant algebraic surfaces and Darboux invariants

We will use the following results (see Theorem 8.7 and Proposition 8.4 of [3], respectively, for a proof):

Proposition 2.2. *Assume that a system (1.1) admit p irreducible invariant algebraic surfaces $f_i = 0$ with cofactors K_i, for $i = 1, \cdots, p$, not all zero such that $\sum_{i=1}^{p} \lambda_i K_i = -s$ for some $s \in \mathbb{R} \setminus 0$, then the function*

$$f_1^{\lambda_1} \cdots f_p^{\lambda_p} e^{st}$$

is a Darboux invariant of that system.

Proposition 2.3. *Suppose $f \in \mathbb{R}[x,y,z]$ and let $f = f_1^{n_1} \cdots f_r^{n_r}$ be its factorization into irreducible factors over $\mathbb{R}[x,y,z]$. Then, for a polynomial system (1.1), $f = 0$ is an invariant algebraic curve with cofactor K_f if and only if $f_i = 0$ is an invariant algebraic curve for each $i = 1 \cdots, r$ with cofactor K_{f_i}. Moreover $K_f = n_1 K_{f_1} + \cdots + n_r K_{f_r}$.*

The following proposition is Proposition 5 of [8].

Proposition 2.4. *Let $\mathbb{S}^2$ be the infinity of the Poincaré ball and $I(x,y,z,t) = f(x,y,z)\ e^{st}$ be a Darboux invariant of a system (1.1). Let also $p \in \mathbb{R}^3$ and $\phi_p(t)$ be the solution of that system (1.1) with maximal interval (α_p, ω_p) such that $\phi_p(0) = p$. Then*

1. *Assume that $s > 0$. If $\omega_p = +\infty$, then $\omega(p)$ is contained in the closure $\overline{\{f(x,y,z) = 0\}}$ in the Poincaré ball, and if $\alpha_p = -\infty$ then $\alpha(p) \subset \overline{\{f(x,y,z) = 0\}} \cap \mathbb{S}^2$, being $\mathbb{S}^2$ the boundary of the Poincaré ball.*

2. *Assume that $s < 0$. If $\alpha_p = -\infty$, then $\alpha(p)$ is contained in $\overline{\{f(x,y,z) = 0\}}$, and if $\omega_p = +\infty$, then $\omega(p) \subset \overline{\{f(x,y,z) = 0\}} \cap \mathbb{S}^2$.*

The following definition and theorem is Definition 3.1 and Theorem 3.2 in [2] (based on the work in [5]).

Let ϕ_t be a smooth flow on a manifold M and suppose C is a submanifold of M consisting entirely of equilibrium points for the flow. C is said to be *normally hyperbolic* if the tangent bundle to M over C splits into three subbundles TC, E^s, and E^u that are invariant under $d\phi_t$

and satisfy: $d\phi_t$ contracts E^s exponentially, $d\phi_t$ expands E^u exponentially and TC is the tangent bundle of C.

For normally hyperbolic submanifolds one has the usual existence of smooth stable and unstable manifolds together with the persistence of these invariant manifolds under small perturbations. More precisely, we have the following theorem.

Theorem 2.5. *Let C be a normally hyperbolic submanifold of equilibrium points for ϕ_t. Then there exist smooth stable and unstable manifolds tangent along C to $E^s \oplus TC$ and $E^u \oplus TC$ respectively. Furthermore, both C and the stable and unstable manifolds are persistent under small perturbations of the flow.*

3 Proof of Propositions 1.1, 1.2, 1.3, 1.5 and Corollary 1.4

3.1 Proof of Proposition 1.1

Let $F(x,y,z) = a_0 + a_1x + a_2y + a_3z + a_4x^2 + a_5xy + a_6xz + a_7y^2 + a_8yz + a_9z^2$ with $a_i \in \mathbb{R}$ and $K = K(x,y,z) = k_0 + k_1x + k_2y + k_3z$ with $k_i \in \mathbb{R}$. If $F(x,y,z) = 0$ is an invariant algebraic surface of a system (1.1), with fixed $\alpha, \beta, \kappa, \lambda \in \mathbb{R}$, with cofactor K it must verify

$$\frac{\partial F}{\partial x}(x(y-1) - \beta z) + \frac{\partial F}{\partial y}(\alpha(1-x^2) - \kappa y) + \frac{\partial F}{\partial z}(x - \lambda z) = (k_0 + k_1x + k_2y + k_3z)F. \tag{3.1}$$

Equating the coefficients of the left-hand side polynomial of (3.1) with the right-hand side polynomial of (3.1) we get a system of 20 equations with 18 unknowns which are a_j for $j = 0, \ldots, 9$, k_i for $i = 0, \ldots, 3$ and α, β, λ and κ. Solving this system of equations with the help of an algebraic manipulator as Mathematica or Maple we obtain the 13 invariant algebraic surfaces F_k given in Table 1.1. This completes the proof of the proposition.

3.2 Proof of Proposition 1.2

We note that if H is a first integral then $H +$ constant is also a first integral. Without loss of generality we can assume that H has no constant term. Moreover, if H is a first integral then CH, where C is a constant, is also a first integral, so the first integrals in Table 1.2 are determined up to multiplication by a constant.

Since a polynomial first integral is an invariant algebraic surface with zero cofactor, from Proposition 1.1, Table 1.1 and Proposition 2.3, Proposition 1.2 is proved. In particular we need to take among the invariant algebraic surfaces in Table 1.1 with zero cofactor also all possible combinations of the invariant algebraic surfaces in Table 1.1 with the respectively non-zero cofactors such that the sum of the cofactors is zero. Thus we obtain the polynomial first integrals F_1, F_2, F_3 and F_6F_7 when $\alpha = \beta = \lambda = \kappa = 0$. Since the constants a, b, c are arbitrary and we look for simple polynomial first integrals, the first integral F_2 becomes the simple first integral $H_1 = y$, and the first integral F_1 is function of the simple first integrals H_1 and $H_2 = x + z - yz$. Moreover F_6F_7 when $\alpha = \beta = \lambda = \kappa = 0$ can be expressed as a function of H_1 and H_2. This completes the proof of the proposition.

3.3 Proof of Proposition 1.3

Since a rational first integral is the quotient of two invariant algebraic surfaces with the same cofactor, Table 1.3 follows from Proposition 1.1, Table 1.1 and Proposition 2.3, taking all possible combinations of the invariant algebraic surfaces in Table 1.1 with the respectively cofactors

and the resulting function is a non-polynomial rational function. To that end, it is taken into account that the sum of invariant surfaces is an invariant surface if the cofactors of both are the same, and also that the product of invariant surfaces is always an invariant surface, with its cofactor being the sum of the corresponding cofactors associated with each of them. Doing so, all possible rational first integrals are: F_{13}/F_4, F_6/F_5, F_{12}/F_8, F_{12}/F_{11}, F_9F_{10}/F_{12}, F_5F_6/F_8, F_5F_6/F_{12}, F_8/F_5^2, F_{12}/F_5^2, F_9F_{10}/F_5^2, F_8/F_6^2, F_{12}/F_6^2. However the unique real simple rational first integral of degree one or two are G_1 (which is obtained from F_8/F_5^2) and G_2 (which is obtained from F_6/F_5) because for the others, they are either polynomial first integrals or can be expressed as a function of G_1 and G_2.

3.4 Proof of Corollary 1.4

From Table 1.2 it follows that system (1.1) under the conditions $\alpha = \beta = \kappa = \lambda = 0$ have the two polynomial first integrals H_1 and H_2. They clearly are independent because H_1 does not depend on x or z while H_2 does depend on these variables. This proves Corollary 1.4.

3.5 Proof of Proposition 1.5

It follows from Propositions 2.2 and 2.3 that to obtain Table 1.4 we need to take all the invariant algebraic surfaces in Table 1.1 such that their cofactors are non-zero constants, or different invariant algebraic surfaces with nonzero constant cofactor such that the product of them to some power (either positive or negative) provide a polynomial or a rational function $f(x,y,z)$ with constant cofactor $-s$, and consequently a Darboux invariant $f(x,y,z)e^{st}$.

The Darboux invariants I_1, I_2, I_3, I_4 and I_6, of Table 1.4 are simple and are obtained from the invariant algebraic surfaces of Table 1.1 as $I_1 = F_5e^{\kappa t}$, $I_1 + I_2 = F_6e^{\kappa t}$, $I_3 = F_7e^{-\kappa t}$, $I_4 + I_1^2 = F_8e^{2\kappa t}$ and $I_6 = F_{12}e^{-\kappa t}$. Moreover, I_5 is a simple Darboux invariant: it is $I_5 = F_{11}e^{2\kappa t}$ if $\kappa(1-\kappa) > 0$, and it is $I_5 = F_9F_{10}e^{2\kappa t}$ if $\kappa(1-\kappa) < 0$.

4 Proof of Theorem 1.6

The family of systems (1.1) under conditions $\alpha = 0$, $\beta = \kappa = -\lambda$ has the first integral $H_2 = x + z - yz$, so on any level $H_2 = h$ we can reduce these systems to the planar polynomial family of systems

$$\dot{y} = -\kappa y, \quad \dot{z} = h + (\kappa - 1)z + yz. \tag{4.1}$$

In this section we study the dynamics of systems (4.1) in the Poincaré disc for any value of $h \in \mathbb{R}$.

Finite equilibrium points

If $\kappa \neq 1$ and $\kappa \neq 0$ systems (4.1) have the unique equilibrium point $(0, h/(1-\kappa))$ which is a stable hyperbolic node if $\kappa \in (0,1)$, an a hyperbolic saddle if $\kappa > 1$ or $\kappa < 0$.

If $\kappa = 1$ and $h = 0$ then system (4.1) has the straight line $y = 0$ filled of equilibrium points. If $\kappa = 1$ and $h \neq 0$ there are no finite equilibrium points on systems (4.1).

If $\kappa = 0$ and $h \neq 0$ then systems (4.1) have the curve $z = h/(1-y)$ filled with equilibrium points. If $\kappa = 0$ and $h = 0$ then system (4.1) has two curves filled with equilibrium points: $z = 0$ and $y = 1$.

When $\kappa = 1$ and $h = 0$ system (4.1) becomes

$$\dot{y} = -y, \quad \dot{z} = yz,$$

and the orbits behave as in Figure 4.1, so the equilibrium points are all stable.

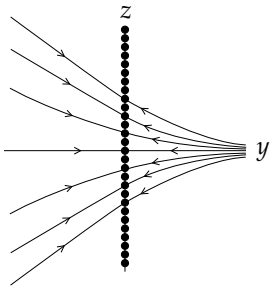

Figure 4.1: Phase portrait around the line $y = 0$ consisting of equilibrium points.

When $\kappa = 0$ systems (4.1) become

$$\dot{y} = 0, \quad \dot{z} = h - z + yz,$$

so all the orbits live in vertical straight lines: if $h > 0$ the orbits are as in Figure 4.2(a), if $h = 0$ then the phase portrait becomes as in Figure 4.2(b), and finally if $h < 0$ the orbits are as in Figure 4.2(c).

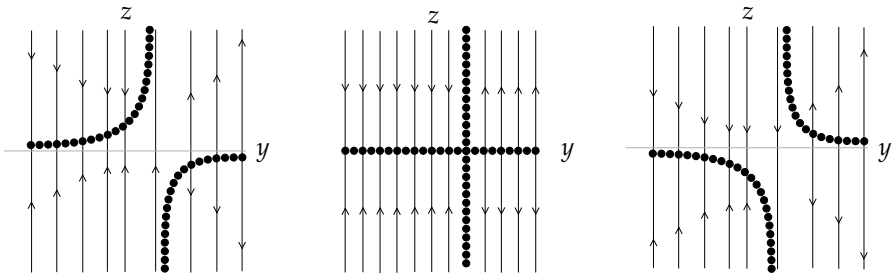

(a) $h > 0$ (b) $h = 0$ (c) $h < 0$

Figure 4.2: Finite phase portraits of systems (4.1) with $\kappa = 0$.

Infinite equilibrium points

In order to study the dynamics of systems (4.1) at infinity, we will use the Poincaré compactification introduced in subsection 2.1.1. We only consider the case $\kappa \neq 0$, as the phase portrait in the case $\kappa = 0$ can be totally determined with the finite phase portrait.

In the local chart U_1 systems (4.1) have the expression

$$\dot{u} = u + (2\kappa - 1)uv + hv^2, \quad \dot{v} = \kappa v^2. \tag{4.2}$$

If $\kappa \neq 0$, the only equilibrium point at infinity is the origin of the systems. This point is a semi-hyperbolic equilibrium point. Applying Theorem 2.19 of [3] it is a saddle-node for any $\kappa \neq 0$.

In the local chart U_2 systems(4.1) have the expression

$$\dot{u} = -u^2 - (2\kappa - 1)uv - huv^2, \quad \dot{v} = -uv - (\kappa - 1)v^2 - hv^3. \tag{4.3}$$

The only point we need to study in the local chart U_2 is the origin, and it is linearly zero.

We will study the local phase portrait at the origin of the chart U_2 doing vertical blow-ups. Since the characteristic directions at the origin of system (4.3) are given by the factors of the polynomial $\kappa u(v-2)v^2 = 0$ when $\kappa \neq 0$, we need to do a twist $(u, v) = (u_1 - v_1, v_1)$ because $u = 0$ is a characteristic direction. When $\kappa = 0$ all the directions are characteristic. In the new coordinates (u_1, v_1) system (4.3) becomes

$$\dot{u_1} = -u_1^2 + 2(1-\kappa)u_1v_1 + \kappa v_1^2 - hu_1v_1^2, \quad \dot{v_1} = -v_1(u_1 + (\kappa - 2)v_1 + hv_1^2). \tag{4.4}$$

Now we do the vertical blow up $(u_1, v_1) = (u_2, u_2v_2)$ and system (4.4) becomes

$$\dot{u_2} = -u_2^2(1 + 2(\kappa - 1)v_2 - \kappa v_2^2 + hu_2v_2^2), \quad \dot{v_2} = -\kappa u_2(v_2 - 1)v_2^2. \tag{4.5}$$

Since u_2 is a common factor of $\dot{u_2}$ and $\dot{v_2}$ we rescale the time and we get the differential system

$$\dot{u_2} = -u_2(1 + 2(\kappa - 1)v_2 - \kappa v_2^2 + hu_2v_2^2), \quad \dot{v_2} = -\kappa(v_2 - 1)v_2^2. \tag{4.6}$$

This system has on the straight line $u_2 = 0$ two equilibrium points: $(0, 0)$ and $(0, 1)$. As $\kappa \neq 0$ by Theorem 2.19 of [3] the point $(0, 0)$ is a saddle-node.

If $\kappa < 0$ the point $(0, 1)$ is a hyperbolic unstable node, and if $\kappa \in (0, 1)$ it is a hyperbolic saddle, if $\kappa = 1$ it is a semihyperbolic saddle node if $h \neq 0$ and it is not isolated if $h = 0$, and if $\kappa > 1$ it is a hyperbolic stable node.

Assume $\kappa < 0$. Then for system (4.6) the origin is a saddle-node and the point $(0, 1)$ is an unstable node, and in Figure 4.3(a) we include the local phase portrait of this system in a neighborhood of the straight line $u_2 = 0$. If we multiply by u_2 to return to system (4.5), then all points on the u_2-axis become equilibrium points, and the orientation of the orbits in the second and third quadrants are reversed. Thus we obtain the phase portrait of Figure 4.3(b) for system (4.5) around the straight line $u_2 = 0$. Now we undo the blow up to obtain the local phase portrait at the origin of system (4.4). We must take into account that for this system the u_1-axis is invariant and as $\dot{u_1}|_{u_1=0} = -u_1^2$, then over this axis the flow points in the negative direction. The v_1-axis is not invariant, and we have that $\dot{u_1}|_{u_1=0} = kv_1^2$ and $\dot{v_1}|_{u_1=0} = (2-k)v_1^2 - hv_1^3$, so in a neighborhood of the origin, over the v_1 axis, the flow points in the negative u_1-direction and in the positive v_1-direction. Then we obtain the local phase portrait in Figure 4.3(c) for system (4.4) . Finally, if we undo the twist, we obtain the local phase portrait at the origin of the local chart U_2, which is given in Figure 4.3(d).

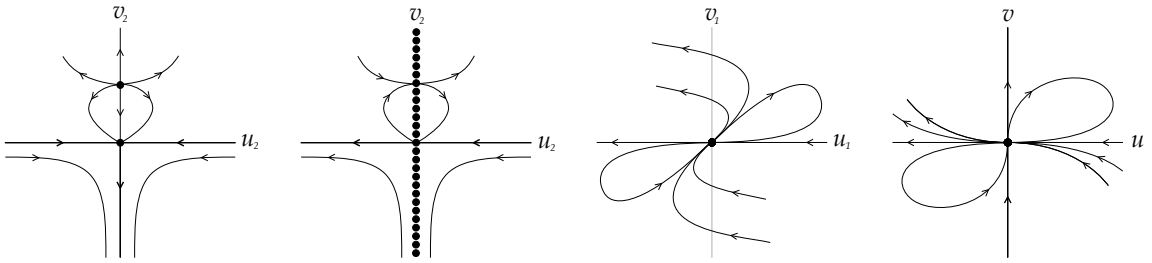

(a) (b) (c) (d)

Figure 4.3: Blowing down of the origin of system (4.3) with $\kappa < 0$.

Assume now that $\kappa \in (0,1)$. In Figure 4.4(a) we plotted the local phase portrait of system (4.6) in a neighborhood of the straight line $u_2 = 0$. In Figure 4.4(b) there is the phase portrait of system (4.5) around the straight line $u_2 = 0$ and in Figure 4.4(c) at the origin of system (4.4). Finally in Figure 4.4(d) there is the local phase portrait at the origin of the local chart U_2.

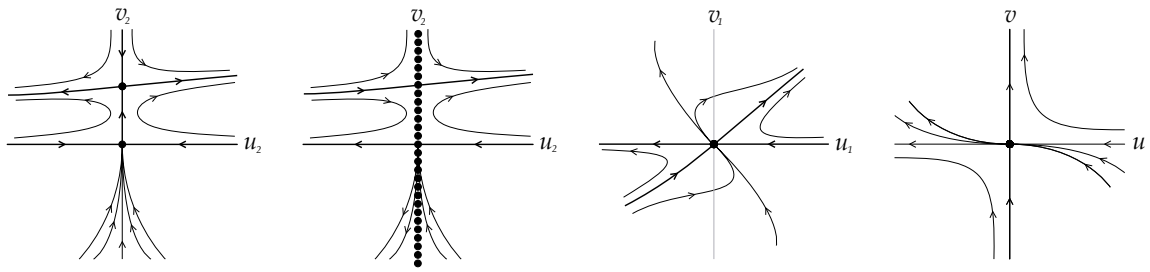

(a) (b) (c) (d)

Figure 4.4: Blowing down of the origin of the system (4.3) with $\kappa \in (0,1)$.

For $\kappa = 1$ and $h > 0$, in Figure 4.5(a) we plotted the local phase portrait of system (4.6) in a neighborhood of the straight line $u_2 = 0$. In Figure 4.5(b) there is the phase portrait of system (4.5) around the straight line $u_2 = 0$ and in Figure 4.5(c) at the origin of system (4.4). Finally in Figure 4.5(d) there is the local phase portrait at the origin of the local chart U_2.

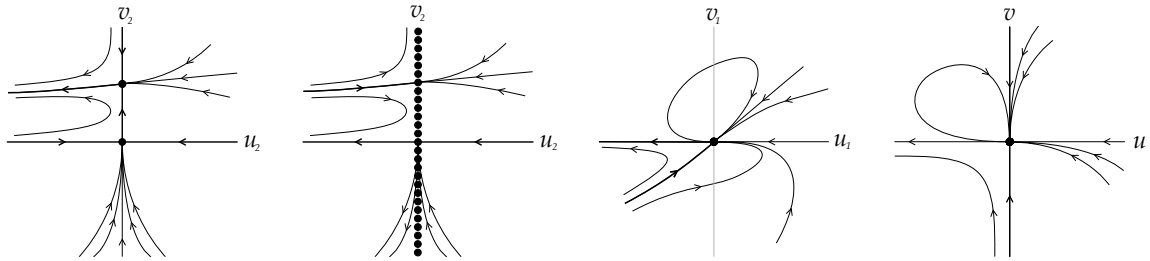

(a) (b) (c) (d)

Figure 4.5: Blowing down of the origin of the system (4.3) with $\kappa = 1$ and $h > 0$.

Assume that $\kappa = 1$ and $h < 0$. In Figure 4.6(a) we plotted the local phase portrait of system (4.6) in a neighborhood of the straight line $u_2 = 0$. In Figure 4.6(b) there is the phase portrait of system (4.5) around the straight line $u_2 = 0$ and in Figure 4.6(c) at the origin of system (4.4). Finally in Figure 4.6(d) there is the local phase portrait at the origin of the local chart U_2.

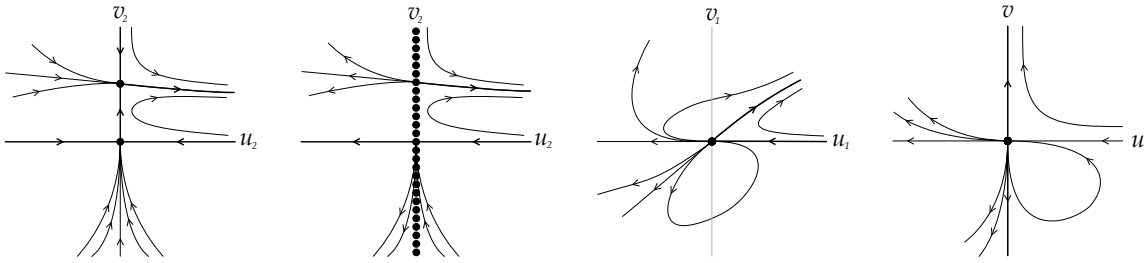

(a) (b) (c) (d)

Figure 4.6: Blowing down of the origin of the system (4.3) with $\kappa = 1$ and $h < 0$.

If $\kappa = 1$ and $h = 0$, the line $u = 0$ is filled of equilibrium points. We eliminate the common factor u rescaling the time and we get the differential system

$$\dot{u} = -u - v, \qquad \dot{v} = -v. \tag{4.7}$$

The local phase portrait of system (4.7) is shown in Figure 4.7(a), and the local phase portrait at the origin of U_2 is given in Figure 4.7(b).

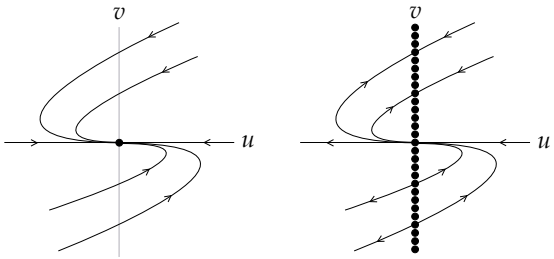

(a) (b)

Figure 4.7: Phase portrait at the origin of the system (4.3) with $\kappa = 1$ and $h = 0$.

Finally, for $\kappa > 1$, in Figure 4.8(a) we plotted the local phase portrait of system (4.6) in a neighborhood of the straight line $u_2 = 0$. In Figure 4.8(b) there is the phase portrait of system (4.5) around the straight line $u_2 = 0$ and in Figure 4.8(c) at the origin of system (4.4). Finally in Figure 4.8(d) there is the local phase portrait at the origin of the local chart U_2.

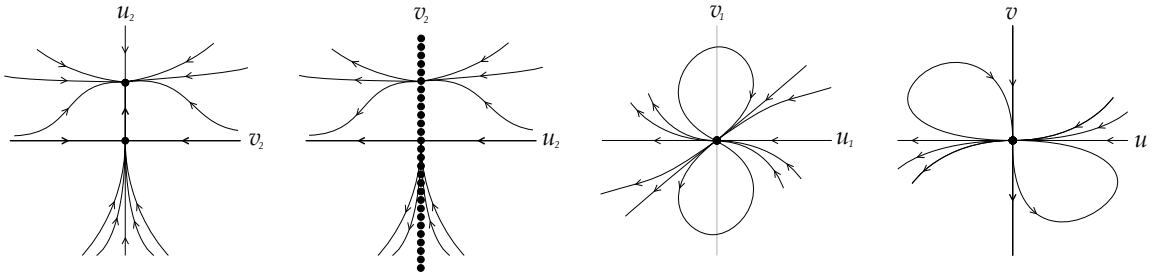

(a) (b) (c) (d)

Figure 4.8: Blowing down of the origin of the system (4.3) with $\kappa \in (1, 2)$.

Summarizing, all the possible phase portraits at the origin of the local chart U_2 for $k \neq 0$, are given in Figure 4.9.

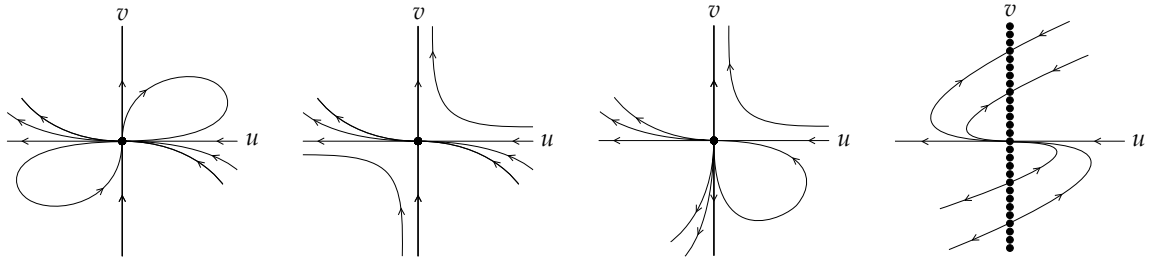

$L_1\ (\kappa < 0)$ $L_2\ (\kappa \in (0,1))$ $L_3\ (\kappa = 1,\ h < 0)$ $L_4\ (\kappa = 1,\ h = 0)$

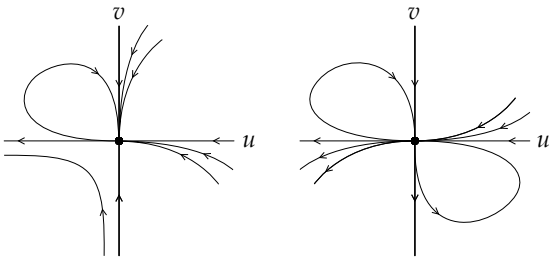

$L_5\ (\kappa = 1,\ h > 0)$ $L_6\ (\kappa > 1)$

Figure 4.9: Phase portraits of the origin of U_2.

4.1 Phase portraits in the Poincaré disc

In this subsection we give the topological classification of all phase portraits of systems (4.1) stated in Theorem 1.6.

We bring together the local information previously obtained. In some cases the local information gives rise to only one phase portrait in the Poincaré disc, this occurs when the separatrices can be connected in only one way, but in other cases several phase portraits in the Poincaré disc are possible, and we shall prove which of them are feasible.

Case $\kappa = 0$. In this case there exists a continuum of equilibrium points given by the curve $z = h/(1-y)$, and the finite phase portrait completely defines the phase portrait in the Poincaré disc. The infinite equilibrium points are also contained in this continuum. All the orbits in the finite region are contained in vertical straight lines. We will have three different phase portraits depending on whether $h > 0$, $h = 0$ or $h < 0$, because the sign of h determines the position of the continuum of equilibria and the orientation of the orbits. In the case in which h is zero, the curve of equilibrium points previously mentioned becomes the y-axis, and we have another straight line filled of equilibrium points, which is $y = 1$. The three possibilities are given in Figure 4.10. Cases with $h > 0$ and $h < 0$ are topologically equivalent by doing a symmetry with respect to the y-axis, so in the classification it is enough to consider one of them, which is G1 in Figure 1.1. The case with $h = 0$ is G2 in Figure 1.1.

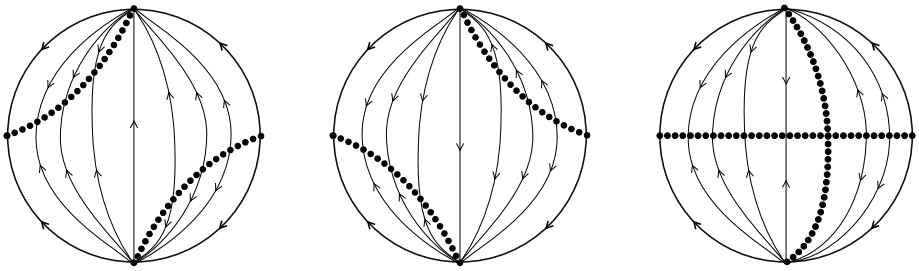

$h > 0$ $h < 0$ $h = 0$

Figure 4.10: Possible phase portraits of systems (4.1) with $\kappa = 0$.

Case $\kappa \in (0,1)$. In this case there exist the finite equilibrium point P which is a stable node, the origin of U_1 is a saddle-node and the origin of U_2 has the local phase portrait L_2. We recall that the origin of the local charts V_1 and V_2 have the same phase portraits as the origin of the local charts U_1 and U_2, respectively, but reversing the orientation of the orbits. Then, we obtain only one possible phase portrait, which is G3 in Figure 1.1. Note that in the figure the point P is represented in the positive part of the z-axis, which corresponds to $h > 0$. For the case $h < 0$ the point is over the negative part of the z-axis, but these phase portraits are topologically equivalent.

Case $\kappa = 1$, $h \neq 0$. There are not finite equilibrium points, the origin of U_1 has the local phase portrait L_{11} and the origin of U_2 has the local phase portrait L_{24} if $h > 0$, and L_{25} if $h < 0$. In both cases there are only one way to connect the separatrices. In the case $h > 0$ we obtain the global phase portrait G4 in Figure 1.1, and in the case $h < 0$ we obtain a topologically equivalent phase portrait, obtained by a symmetry with respect to the y-axis.

Case $\kappa = 1$, $h = 0$. The z-axis is a continuum of equilibrium points, and then the origin of charts U_2 and V_2 are contained in this continuum, and the finite orbits are as in Figure 4.1. The origin of chart U_1 has the local phase portrait L_{11}. There is only one possible global configuration in this case, which is G5 in Figure 1.1.

Case $\kappa > 1$. In this case the finite equilibrium point P is a saddle, the origin of U_1 is a saddle-node and the origin of U_2 has the local phase portrait L_6.

We first consider $h > 0$. The separatrices can be connected in three ways, giving rise to the three phase portraits given in Figure 4.11.

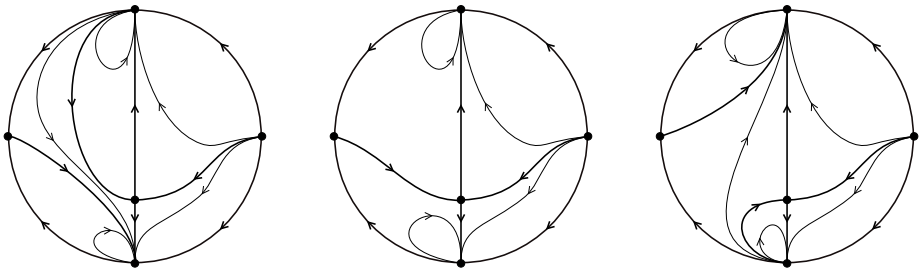

Case 1 Case 2 Case 3

Figure 4.11: Possible phase portraits of systems (4.1) with $\kappa > 1$, $h > 0$.

We can prove that the two first cases of Figure 4.11 are not possible. The flow over the horizontal axis points upward as $\dot{z}|_{z=0} = h > 0$. In Figure 4.12 we can see two shaded regions. In the shaded region of case 1 the flow points downwards over the horizontal axis, so that configuration is not possible. If we take any point in the shaded region of case 2, the orbit passing through that point starts and ends in the origin of the local chart U_2, so at some point of the z-axis the flow points downwards, so this case is also not possible. The only possible phase portrait is the one in case 3, which corresponds to G6 in Figure 1.1.

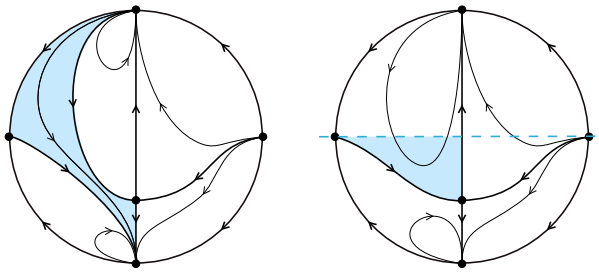

Case 1 Case 2

Figure 4.12: Regions that allow us to prove that the flow points downwards over the z-axis.

For the case with $h < 0$ an analogous reasoning can be done. The obtained phase portrait is topologically equivalent to G6 by doing a symmetry with respect to the y-axis.

Case $\kappa < 0$. As in the previous case, the finite equilibrium point P is a saddle, but the origin of U_1 is a saddle-node, and the origin of U_2 has the local phase portrait L_1.

We consider $h > 0$. We can connect the separatrices in three forms, giving rise to the three phase portraits given in Figure 4.13.

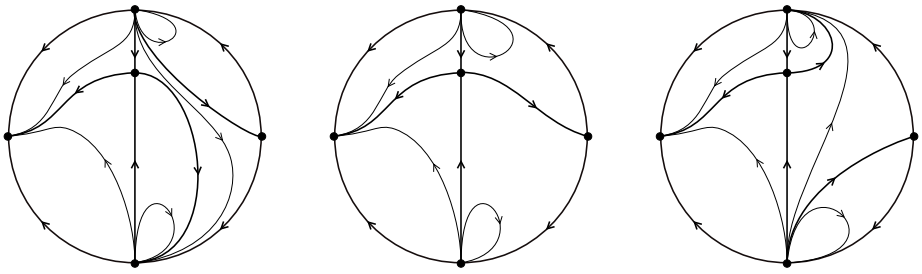

Case 1 Case 2 Case 3

Figure 4.13: Possible phase portraits of systems (4.1) with $\kappa < 0$.

Cases 1 and 2 are not possible and an analogous reasoning to the previous case works, as we find that the flow point downwards at some points of the y-axis, which contradicts the fact that $\dot{z}|_{z=0} = h > 0$. The only feasible phase portrait is case 3, which is topologically equivalent to G6 in Figure 1.1, by doing a symmetry with respect to the x-axis, a symmetry with respect to the z-axis and reversing the orientation.

For the case with $h < 0$ we obtain analogous results. The obtained phase portrait is topologically equivalent to case 3 by doing a symmetry with respect to the y-axis.

Summarizing the information in this section, we can conclude that systems (4.1) can present six topologically different phase portraits, given in Figure 1.1 and according to the classification given in Table 4.1.

Conditions	**Phase portrait**
$\kappa = 0,\ h \neq 0$	G1
$\kappa = 0,\ h = 0$	G2
$\kappa \in (0,1)$	G3
$\kappa = 1,\ h \neq 0$	G4
$\kappa = 1,\ h = 0$	G5
$\kappa > 1$	G6
$\kappa < 0$	

Table 4.1: Classification of phase portraits of systems (4.1).

5 Proof of Theorem 1.7

We consider systems (1.1) under conditions $\alpha = \kappa(1-\kappa) \neq 0$, $\beta = 0$, i.e.,

$$\dot{x} = x(y-1), \quad \dot{y} = \kappa(1-\kappa)(1-x^2) - \kappa y, \quad \dot{z} = x - \lambda z. \tag{5.1}$$

These systems have the Darboux invariant $I_5 = ((\kappa - 1 + y)^2 + \kappa(1-\kappa)x^2)e^{2\kappa t}$.

Finite equilibrium points

We study the finite equilibrium points of systems (5.1).

We first consider the case $\kappa(1-\kappa) > 0$ (i.e. $\kappa \in (0,1)$). If $\lambda \neq 0$, the unique equilibrium point is $P_1 = (0, 1-\kappa, 0)$ contained in $F_{11} = 0$. The Jacobian matrix of systems (5.1) at P_1 has eigenvalues $-\kappa$ with multiplicity two and $-\lambda$. Hence, if $\lambda > 0$ it is a local attractor, and if $\lambda < 0$ it has a 2-dimensional stable manifold and a 1-dimensional unstable manifold. If $\lambda = 0$ then the straight line $(0, 1-\kappa, z)$ with $z \in \mathbb{R}$ is filled of equilibria. The eigenvalues of the Jacobian matrix at any of these points are $-\kappa$ with multiplicity two and 0. All equilibrium points are normally hyperbolic and in view of Theorem 2.5 taking into account that in this case we have $\kappa \in (0,1)$ we get that to each equilibrium point arrives a 2-dimensional stable manifold.

Consider now the case $\kappa(1-\kappa) < 0$ (i.e. $\kappa < 0$ or $\kappa > 1$). If $\lambda \neq 0$ there are three equilibrium points which are

$$P_1 = (0, 1-\kappa, 0), \quad P_2 = \Big(\sqrt{\frac{\kappa}{\kappa-1}}, 1, \frac{1}{\lambda}\sqrt{\frac{\kappa}{\kappa-1}}\Big), \quad P_3 = -\Big(\sqrt{\frac{\kappa}{\kappa-1}}, -1, \frac{1}{\lambda}\sqrt{\frac{\kappa}{\kappa-1}}\Big).$$

All three equilibrium points are contained in $F_9 F_{10} = 0$. The eigenvalues of the Jacobian matrix at the equilibrium point P_1 are $-\kappa$ with multiplicity two and $-\lambda$. Hence, P_1 is a local attractor if $\kappa > 1$ and $\lambda > 0$; has a 2-dimensional stable manifold and a 1-dimensional unstable manifold if $\kappa > 1$ and $\lambda < 0$; it is a local repeller if $\kappa, \lambda < 0$, and it has a 2-dimensional

unstable manifold and a 1-dimensional stable manifold if $\kappa < 0$ and $\lambda > 0$. On the other hand the eigenvalues of the Jacobian matrix at the equilibrium points P_2 and P_3 are $-\lambda$, -2κ and κ. Therefore, both equilibrium points have a 2-dimensional stable manifold and a 1-dimensional unstable manifold if either $\kappa > 1$ and $\lambda > 0$, or $\kappa < 0$ and $\lambda > 0$; and they have a 2-dimensional unstable manifold and a 1-dimensional stable manifold if either $\kappa, \lambda < 0$, or $\kappa > 1$ and $\lambda < 0$.

Conditions	**Finite equilibrium points**
$\kappa \in (0,1)$, $\lambda > 0$	P_1 stable node
$\kappa \in (0,1)$, $\lambda < 0$	P_1 saddle (stable manifold of dimension 2)
$\kappa > 1$, $\lambda > 0$	P_1 stable node, P_2 and P_3 saddles (stable manifold of dimension 2)
$\kappa > 1$, $\lambda < 0$	P_1 saddle (stable manifold of dimension 2), P_2 and P_3 saddles (unstable manifold of dimension 2)
$\kappa < 0$, $\lambda < 0$	P_1 unstable node, P_2 and P_3 saddles (unstable manifold of dimension 2)
$\kappa < 0$, $\lambda > 0$	P_1 saddle (unstable manifold of dimension 2), P_2 and P_3 saddles (stable manifold of dimension 2)

Table 5.1: Local behavior of the finite equilibrium points of systems (5.1) with $\lambda \neq 0$.

If $\lambda = 0$ the straight line $(0, 1-\kappa, z)$ with $z \in \mathbb{R}$ is filled of equilibria. The eigenvalues of the Jacobian matrix at any of these points are $-\kappa$ with multiplicity two and 0. All equilibrium points are normally hyperbolic and in view of Theorem 2.5 we have that if $\kappa > 1$ then to each equilibrium point arrives a 2-dimensional stable manifold, and if $\kappa < 0$ at each equilibrium point starts a 2-dimensional unstable manifold.

Dynamics on the invariant surfaces

We consider two different cases: $\kappa(1-\kappa) > 0$ and $\kappa(1-\kappa) < 0$.

Case $\kappa(1-\kappa) > 0$

In this case $F_{11} = 0$ corresponds to the straight line $(0, 1-\kappa, z)$ with $z \in \mathbb{R}$. The dynamics on this straight line is given by $\dot{z} = -\lambda z$.

If $\lambda > 0$ the points over this straight line have their α-limit at the endpoints of the z-axis in the sphere, and their ω-limit in P_1. If $\lambda < 0$ the points over this straight line have their α-limit at P_1 and their ω-limit at the endpoints of the z-axis in the sphere. This is represented in Figure 5.1. Note that if $\lambda = 0$ the straight line is filled with equilibria.

Case $\kappa(1-\kappa) < 0$

We will study the dynamics on $F_9 = 0$ and on $F_{10} = 0$.

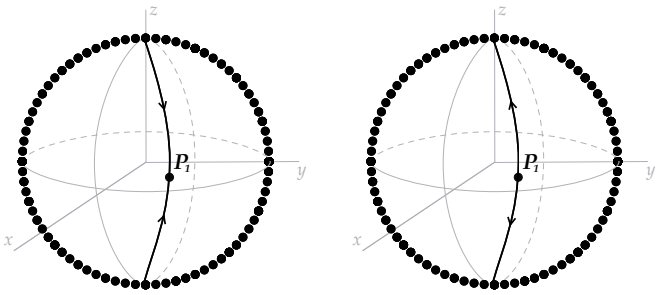

$\lambda > 0$ $\lambda < 0$

Figure 5.1: Phase portraits in the Poincaré disc for systems (5.2) and (5.3).

Dynamics on $F_9 = 0$

We note that systems (5.1) restricted to $F_9 = \kappa - 1 - \sqrt{\kappa(\kappa-1)}x + y = 0$ by setting $y = 1 - \kappa + \sqrt{\kappa(\kappa-1)}x$ are

$$\dot{x} = x\left(\sqrt{\kappa(\kappa-1)}x - \kappa\right), \quad \dot{z} = x - \lambda z. \tag{5.2}$$

When $\lambda \neq 0$, there are two equilibrium points $Q_1 = (0,0)$ and $Q_2 = \frac{\sqrt{\kappa(\kappa-1)}}{\kappa-1}(1, 1/\lambda)$. The eigenvalues of the Jacobian matrix at Q_1 are $-\kappa$, $-\lambda$ and the eigenvalues of the Jacobian matrix at Q_2 are κ and $-\lambda$. Hence, Q_1 is a stable node when $\kappa, \lambda > 0$; an unstable node when $\kappa, \lambda < 0$, and a saddle when $\kappa\lambda < 0$. On the other hand Q_2 is a stable node when $\kappa < 0$ and $\lambda > 0$; an unstable node when $\kappa > 0$ and $\lambda < 0$, and a saddle when $\kappa\lambda > 0$.

If $\lambda = 0$ then $x = 0$ is filled with equilibrium points. Removing the common factor x between $\dot{x}$ and $\dot{z}$ with a rescaling of the time we get that system (5.2) when $\lambda = 0$ becomes

$$\dot{x} = \sqrt{\kappa(\kappa-1)}x - \kappa, \quad \dot{z} = 1. \tag{5.3}$$

This linear system has the phase portrait in Figure 5.2(a) for $k > 0$, and so system (5.2) with $\lambda = 0$ has the phase portrait in Figure 5.2(b) for $k > 0$. In the cases with $k < 0$ the phase portrait is the same but doing a symmetry with respect to the z-axis and changing the time t into $-t$.

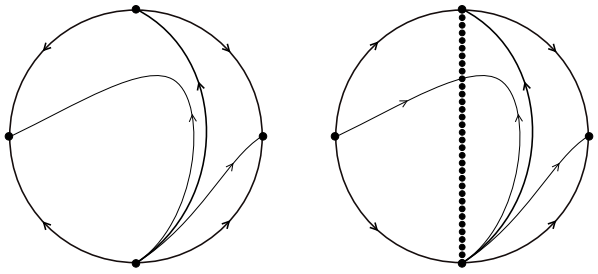

(a) (b)

Figure 5.2: Phase portraits in the Poincaré disc for systems (5.2) and (5.3).

From now on we focus on the study of system (5.2) with $\lambda \neq 0$. Note that system (5.2) has the invariant straight lines $x = 0$ and $\sqrt{\kappa(\kappa-1)}x - \kappa = 0$ that contain the equilibrium points. Therefore there cannot be periodic orbits.

Now we study system (5.2) in the Poincaré disc. We first study it on the local chart U_1. On the local chart U_1 system (5.2) takes the form

$$\dot{u} = -\sqrt{\kappa(\kappa-1)}u + v + (\kappa-\lambda)uv, \quad \dot{v} = v(-\sqrt{\kappa(\kappa-1)} + \kappa v).$$

The unique equilibrium point on $v = 0$ is the origin $(0,0)$. The Jacobian matrix at that point has the eigenvalue $-\sqrt{\kappa(\kappa-1)}$ with multiplicity two and so the origin of the local chart U_1 is a stable node.

On the local chart U_2 system (5.2) takes the form

$$\dot{u} = u\left(\sqrt{\kappa(\kappa-1)}u + (\lambda-\kappa)v - uv\right), \quad \dot{v} = v^2(\lambda-u). \tag{5.4}$$

The origin is an equilibrium point. The Jacobian matrix at that point is the zero matrix, so in order to study its local phase portrait we need to do blow-ups. Since the characteristic directions at the origin of system (5.4) are given by the factors of the polynomial $uv(\sqrt{\kappa(\kappa-1)}u - \kappa v) = 0$, we need to do a twist $(u,v) = (u_1 - v_1, v_1)$ because $u = 0$ is a characteristic direction. In the new coordinates (u_1, v_1) system (5.4) becomes

$$\begin{aligned} \dot{u_1} &= \sqrt{\kappa(\kappa-1)}u_1^2 - \left(\kappa - \lambda + 2\sqrt{\kappa(\kappa-1)}\right)u_1v_1 + \left(\kappa + \sqrt{\kappa(\kappa-1)}\right)v_1^2 - u_1^2v_1 + u_1v_1^2, \\ \dot{v_1} &= v_1^2(\lambda - u_1 + v_1). \end{aligned} \tag{5.5}$$

Now we do the vertical blow up $(u_1, v_1) = (u_2, u_2v_2)$ and system (5.5) becomes

$$\begin{aligned} \dot{u_2} &= u_2^2\left(\sqrt{\kappa(\kappa-1)} - \left(\kappa - \lambda + 2\sqrt{\kappa(\kappa-1)}\right)v_2 - u_2v_2 + \left(\kappa + \sqrt{\kappa(\kappa-1)}\right)v_2^2 + u_2v_2^2\right), \\ \dot{v_2} &= u_2v_2(v_2-1)\left(\sqrt{\kappa(\kappa-1)} - \left(\kappa + \sqrt{\kappa(\kappa-1)}\right)v_2\right). \end{aligned} \tag{5.6}$$

Since u_2 is a common factor of $\dot{u_2}$ and $\dot{v_2}$ we rescale the time and we get the differential system

$$\begin{aligned} \dot{u_2} &= u_2\left(\sqrt{\kappa(\kappa-1)} - \left(\kappa - \lambda + 2\sqrt{\kappa(\kappa-1)}\right)v_2 - u_2v_2 + \left(\kappa + \sqrt{\kappa(\kappa-1)}\right)v_2^2 + u_2v_2^2\right), \\ \dot{v_2} &= v_2(v_2-1)(\sqrt{\kappa(\kappa-1)} - (\kappa + \sqrt{\kappa(\kappa-1)})v_2). \end{aligned} \tag{5.7}$$

This system has on the straight line $u_2 = 0$ three equilibrium points: $(0,0)$, $(0,1)$ and $\left(0, \frac{\sqrt{\kappa(\kappa-1)}}{\kappa+\sqrt{\kappa(\kappa-1)}}\right)$. The equilibrium point $(0,0)$ is a hyperbolic saddle. The equilibrium point $(0,1)$ is a hyperbolic stable node if $\lambda < 0$ and $\kappa > 0$; a hyperbolic unstable node if $\lambda > 0$ and $\kappa < 0$, and a hyperbolic saddle if $\lambda\kappa > 0$. Finally the equilibrium point $\left(0, \frac{\sqrt{\kappa(\kappa-1)}}{\kappa+\sqrt{\kappa(\kappa-1)}}\right)$ is a hyperbolic saddle if $\lambda\kappa < 0$, a hyperbolic stable node if $\lambda, \kappa < 0$ and a hyperbolic unstable node if $\lambda, \kappa > 0$. The equilibrium point $\left(0, \frac{\sqrt{\kappa(\kappa-1)}}{\kappa+\sqrt{\kappa(\kappa-1)}}\right)$ is greater than the point $(0,1)$ if $\kappa < 0$ and is between the points $(0,0)$ and $(0,1)$ if $\kappa > 1$.

Assume $\kappa < 0$ and $\lambda > 0$, in Figure 5.3(a) we plotted the local phase portrait of system (5.7) in a neighborhood of the straight line $u_2 = 0$. In Figure 5.3(b) there is the phase portrait

of system (5.6) around the straight line $u_2 = 0$ and in Figure 5.3(c) at the origin of system (5.5). Finally in Figure 5.3(d) there is the local phase portrait at the origin of the local chart U_2.

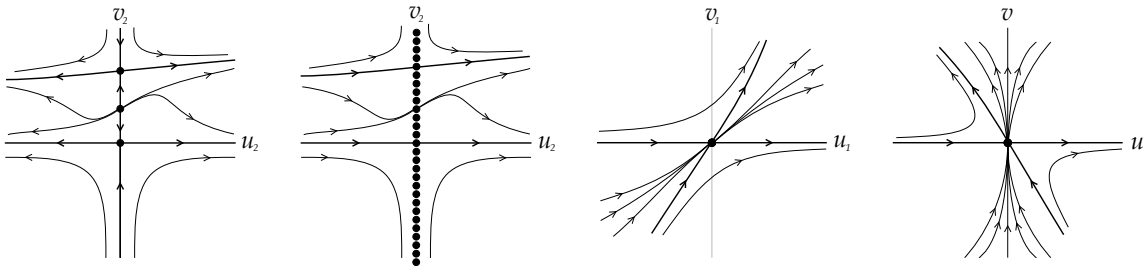

(a) (b) (c) (d)

Figure 5.3: Blowing down of the origin of the system (5.4) with $\kappa < 0$ and $\lambda > 0$.

Now consider $\kappa < 0$ and $\lambda < 0$. In Figure 5.4(a) we plotted the local phase portrait of system (5.7) in a neighborhood of the straight line $u_2 = 0$. In Figure 5.4(b) there is the phase portrait of system (5.6) around the straight line $u_2 = 0$ and in Figure 5.4(c) at the origin of system (5.5). Finally in Figure 5.4(d) there is the local phase portrait at the origin of the local chart U_2.

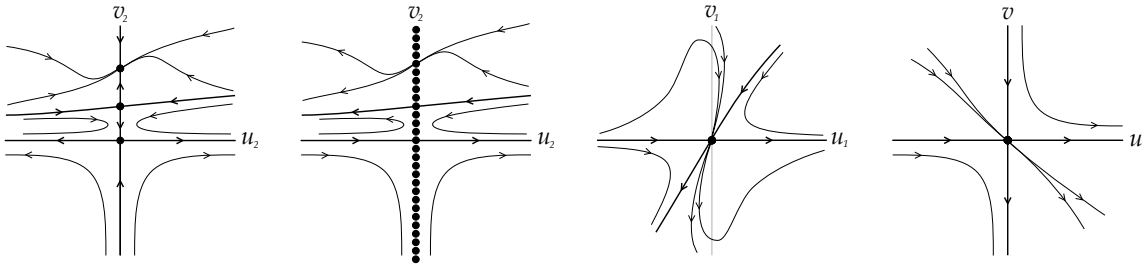

(a) (b) (c) (d)

Figure 5.4: Blowing down of the origin of the system (5.4) with $\kappa < 0$ and $\lambda < 0$.

For $\kappa > 1$ and $\lambda > 0$, in Figure 5.5(a) we plotted the local phase portrait of system (5.7) in a neighborhood of the straight line $u_2 = 0$. In Figure 5.5(b) there is the phase portrait of system (5.6) around the straight line $u_2 = 0$ and in Figure 5.5(c) at the origin of system (5.5). Finally in Figure 5.5(d) there is the local phase portrait at the origin of the local chart U_2.

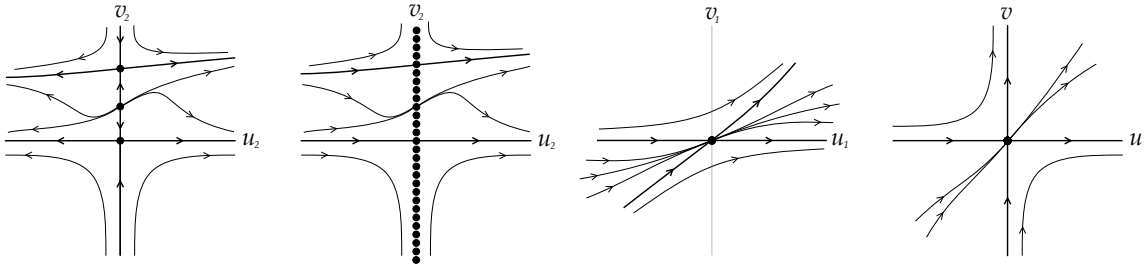

(a) (b) (c) (d)

Figure 5.5: Blowing down of the origin of the system (5.4) with $\kappa > 1$ and $\lambda > 0$.

Consider $\kappa > 1$ and $\lambda < 0$. In Figure 5.6(a) we plotted the local phase portrait of system (5.7) in a neighborhood of the straight line $u_2 = 0$. In Figure 5.6(b) there is the phase portrait of system (5.6) around the straight line $u_2 = 0$ and in Figure 5.6(c) at the origin of system (5.5). Finally in Figure 5.6(d) there is the local phase portrait at the origin of the local chart U_2.

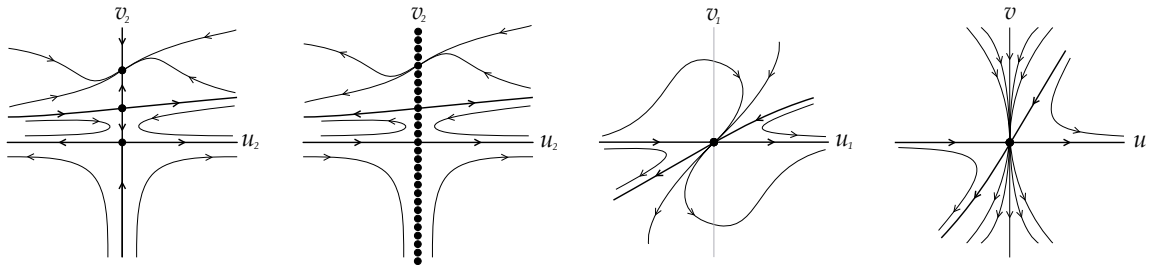

(a) (b) (c) (d)

Figure 5.6: Blowing down of the origin of the system (5.4) with $\kappa > 1$ and $\lambda < 0$.

Phase portraits in the Poincaré disc

Taking into account the local information obtained for the finite and infinite equilibrium points, now we study the local phase portraits in the Poincaré disc. In all the cases the local information gives rise to only one phase portrait, as the separatrices can be connected only in one way.

Case $\lambda > 0$, $k > 0$. In this case the origin is a stable node and the equilibrium point Q_2 is a saddle and it is on the first quadrant. The origin of the local chart U_1 is a stable node and the origin of U_2 has the phase portrait in Figure 5.5(d). The equilibrium point Q_2 is contained in the invariant straight line $\sqrt{\kappa(\kappa-1)}x - \kappa = 0$, and over this line are the two stable separatrices of the saddle Q_2. The unstable separatrices have only one possible ω-limit for each of them: one goes to the origin and the other to the origin of the local chart U_2. Then we have the phase portrait given in Figure 1.2(a).

Case $\lambda > 0$, $k < 0$. In this case the origin is a saddle and the equilibrium point Q_2 is a stable node and it is on the third quadrant. The origin of the local chart U_1 is a stable node and the origin of U_2 has the phase portrait in Figure 5.3(d). The separatrix that leaves the origin in the half of the disc corresponding to the positive x-axis, goes to the origin of U_2. There are three separatrices in the half of the disc corresponding to the negative x-axis, and for the three of them the only possible ω-limit is the equilibrium point Q_2. Then we have a phase portrait which is topologically equivalent to the one in Figure 1.2(a) by moving the equilibrium point Q_2 into the origin and thus the origin into the first quadrant.

Case $\lambda < 0$, $k > 0$. In this case the origin is a saddle and the equilibrium point Q_2 is an unstable node and it is on the fourth quadrant. The origin of the local chart U_1 is a stable node and the origin of U_2 has the phase portrait in Figure 5.6(d). Similar to the previous case, there are three separatrices in the half of the disc corresponding to the positive x-axis whose only possible α-limit is the origin of U_2. The α-limit of the other stable separatrix of the origin is the origin of the local chart V_2. The phase portrait obtained is the one of Figure 1.2(b). It is topologically equivalent to the one of Figure 1.2(a) doing a symmetry with respect to the z-axis and changing t into $-t$, but we include it in order to study the $\alpha-$ and ω-limits.

Case $\lambda < 0$, $k < 0$. In this case the origin is an unstable node and the equilibrium point Q_2

is a saddle and it is on the second quadrant. The origin of the local chart U_1 is a stable node and the origin of U_2 has the phase portrait of Figure 5.4(d). The two unstable separatrices of Q_2 are over the invariant line $\sqrt{\kappa(\kappa-1)}x-\kappa=0$ and the stable separatrices have as α-limit the origin and the origin of the local chart V_2. The phase portrait in this case is topologically equivalent to the one of Figure 1.2(b) by moving the equilibrium point Q_2 into the origin.

Summarizing, we have included four phase portraits in Figure 1.2, attending to the orientations of the orbits, but note that phase portraits (a) and (b) of Figure 1.2 are topologically equivalent, and also phase portraits (c) and (d) are topologically equivalent.

Taking into account these phase portraits we analyze the α- and ω-limits of the orbits in the invariant plane $F_9=0$.

If $\lambda>0$ all the points in the invariant plane have their ω-limit at the point Q_9 or at a point at infinity, and their α-limit at an infinite point, except for the points of the two unstable separatrices of P_9 for which their α-limit is P_9.

If $\lambda<0$ all the points in the invariant plane have their ω-limit at an infinite point, except for the points of the two stable separatrices of Q_9 for which their ω-limit is Q_9. Moreover they have their α-limit at the point P_9 or in a point at infinity.

If $\lambda=0$ and $k>0$ all the points in the invariant plane have their ω-limit at an infinite point or at any point of the straight line filled of equilibria and have their α-limit in a point at infinity.

If $\lambda=0$ and $k<0$ all the points in the invariant plane have their ω-limit in a point at infinity and their α-limit at an infinite point or at any point of the straight line filled with equilibria.

Dynamics on $F_{10}=0$

We note that systems (5.1) restricted to $F_{10}=\kappa-1+\sqrt{\kappa(\kappa-1)}x+y=0$ by setting $y=1-\kappa-\sqrt{\kappa(\kappa-1)}x$ are

$$\dot{x}=-x\left(\sqrt{\kappa(\kappa-1)}x+\kappa\right),\quad \dot{z}=x-\lambda z. \tag{5.8}$$

Doing a study completely analogous to the one carried out to study $F_9=0$, we get that the phase portrait are those included in Figure 1.2.

Dynamics at infinity

Study of the infinity in the local charts U_1 and V_1

The expression of the Poincaré compactification of systems (5.1) in the local chart U_1 is given by

$$\begin{aligned}\dot{u}&=\kappa(\kappa-1)-u^2+(1-\kappa)uw+\kappa(1-\kappa)w^2,\\ \dot{v}&=w-uv+(1-\lambda)vw,\\ \dot{w}&=-w(u-w).\end{aligned}$$

At infinity, i.e. when $w=0$ this system writes as

$$\dot{u}=\kappa(\kappa-1)-u^2,\quad \dot{v}=-uv.$$

We have two different cases.

If $\kappa(1-\kappa) > 0$, there are no infinite equilibrium points in the local chart U_1.

If $\kappa(1-\kappa) < 0$, there are two infinite equilibrium points in the local chart U_1, which are $s_1 = (\sqrt{\kappa(\kappa-1)}, 0)$ and $s_4 = (-\sqrt{\kappa(\kappa-1)}, 0)$. The eigenvalues of the Jacobian matrix at these points are $-2\sqrt{\kappa(\kappa-1)}$ and $-\sqrt{\kappa(\kappa-1)}$ for s_1 and $2\sqrt{\kappa(\kappa-1)}$ and $\sqrt{\kappa(\kappa-1)}$ for s_4. Hence s_1 is a stable node and s_4 is an unstable node, as in Figure 5.7

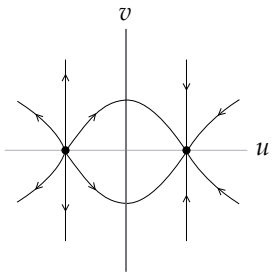

Figure 5.7: Phase portrait at the origin of the local chart U_1 with $\kappa(1-\kappa) < 0$.

Study of the infinity in the local charts U_2 and V_2

The expression of the Poincaré compactification of systems (5.1) in the local chart U_2 is given by

$$\begin{aligned}
\dot{u} &= u(1+\kappa(\kappa-1)w + \kappa(1-\kappa)u^2 + \kappa(\kappa-1)w^2),\\
\dot{v} &= uw + (\kappa-\lambda)vw + \kappa(1-\kappa)u^2v + \kappa(\kappa-1)vw^2,\\
\dot{w} &= \kappa w(w - (\kappa-1)u^2 - (1-\kappa)w^2).
\end{aligned}$$

At infinity, i.e. when $w = 0$ this system writes as

$$\dot{u} = u(1+\kappa(1-\kappa)u^2), \quad \dot{v} = \kappa(1-\kappa)u^3.$$

The line $u = 0$ if filled with equilibria. With a change of time we remove the common factor between $\dot{u}$ and $\dot{v}$ and we get

$$\dot{u} = 1+\kappa(1-\kappa)u^2, \quad \dot{v} = \kappa(1-\kappa)u^2.$$

If $\kappa(1-\kappa) > 0$ there are no equilibrium points and if $\kappa(1-\kappa) < 0$ there are two equilibrium points which are $(\pm 1/\sqrt{\kappa(1-\kappa)}, 0)$. Since we are interested in the equilibrium points with $u = 0$ (the ones with $u \neq 0$ are the same as the ones obtained in the local chart U_1) we do not consider these equilibrium points.

Study of the infinity in the local charts U_3 and V_3

The expression of the Poincaré compactification of systems (5.1) in the local chart U_2 is given by

$$\begin{aligned}
\dot{u} &= u(v + (\lambda-1)w - uw),\\
\dot{v} &= \kappa(\kappa-1)u^2 + (\lambda-\kappa)vw + \kappa(1-\kappa)w^2 - uvw,\\
\dot{w} &= w^2(\lambda-u).
\end{aligned}$$

At infinity, i.e. when $w = 0$ this system writes as

$$\dot{u} = uv, \quad \dot{v} = \kappa(\kappa - 1)u^2.$$

Again the line $u = 0$ if filled with equilibria. With a change of time we remove the common factor between $\dot{u}$ and $\dot{v}$ and we get

$$\dot{u} = v, \quad \dot{v} = \kappa(\kappa - 1)u.$$

We are only interested in the point $(0, 0)$. It is indeed an equilibrium point. Again we consider two cases. If $\kappa(1 - \kappa) > 0$ the origin is a center and if $\kappa(1 - \kappa) < 0$ the origin is a saddle. Going back with the rescaling of time we see that the local phase portraits at the origin of the local chart U_3 are the ones given in Figure 5.8.

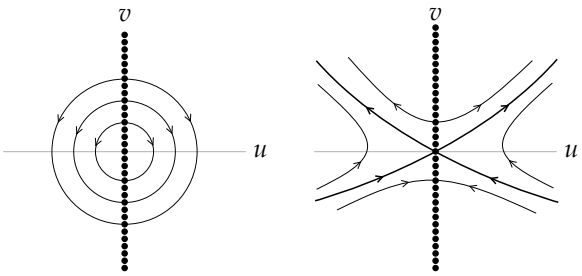

$\kappa(\kappa - 1) < 0$ $\kappa(\kappa - 1) > 0$

Figure 5.8: Phase portraits at the origin of the local chart U_3.

The phase portrait of systems (1.1) under the conditions $\alpha = \kappa(1 - \kappa) \neq 0$ on the sphere at infinity is as shown in Figure 1.3, because the dynamics depend on the sign of $\kappa(1 - \kappa)$.

When $\kappa(\kappa - 1) < 0$ the infinity of the plane $x = 0$ is filled with equilibria. All the orbits are heteroclinic having their α-limit in one of the equilibria with $y > 0$, and their ω-limit in their symmetric equilibria with respect to the origin of coordinates.

When $\kappa(\kappa - 1) > 0$ the infinity of the plane $x = 0$ is again filled with equilibria. There are eight separatrices. The equilibrium points S_3 and S_4 are the α-limits of the two separatrices whose ω-limit is the endpoint of the positive z-axis and also of the two separatrices whose ω-limit is the endpoint of the negative z-axis. On the other hand, the points S_1 and S_2 are the ω-limits of the two separatrices whose α-limit is the endpoint of the positive z-axis and also of the two separatrices whose α-limit is the endpoint of the negative z-axis. The orbits inside the regions delimited by these separatrices have S_4 as α-limit and S_1 as ω-limit (respectively S_3 as α-limit and S_2 as ω-limit). For all the other orbits: the ones with $x, y > 0$ have their α-limit on the infinity of the plane $x = 0$ with $y > 0$ and their ω-limit is S_1; the ones with $x > 0$, $y < 0$ have their ω-limit on the infinity of the plane $x = 0$ with $y < 0$ and their α-limit is S_4; the ones with $x < 0$, $y > 0$ have their α-limit on the infinity of the plane $x = 0$ with $y > 0$ and their ω-limit is S_2; the ones with $x, y < 0$ have their ω-limit on the infinity of the plane $x = 0$ with $y < 0$ and their α-limit is S_3.

α- and ω-limits for the points in $\mathbb{R}^3$

Case $\kappa(\kappa - 1) < 0$

If $\lambda > 0$, all the points in $\mathbb{R}^3$ have their ω-limit in P_1 and their α-limit in a point at infinity.

If $\lambda < 0$ all the points in $\mathbb{R}^3$ have their ω-limit in the endpoints of the z-axis, and their α-limit is an infinite point except for the points at the straight line $(0, 1-k, z)$ with $z \in \mathbb{R}$, for which their α-limit is P_1.

If $\lambda = 0$ all the points in $\mathbb{R}^3$ have their ω-limit in one of the points of the straight line $(0, 1-k, z)$ with $z \in \mathbb{R}$, which is filled with equilibria. Moreover the α-limit is a point at infinity.

Case $\kappa(\kappa - 1) > 0$

If $\lambda > 0$ and $\kappa > 1$ there are three finite equilibrium points, P_1 which is a stable node and P_2 and P_3 which are saddles with a stable manifold of dimension two, one of them in $F_9 = 0$ and the other in $F_{10} = 0$. Taking into account the phase portrait over these invariant surfaces (see Figure 1.2), there are two stable manifolds of dimension one that enter in the invariant surface $F_9 = 0$ and another two that enter into $F_{10} = 0$. The possible α-limits are the negative endpoint of the x-axis in $F_9 = 0$ and the positive endpoint of the x-axis in $F_{10} = 0$, which correspond to the infinite points S_3 and S_4; the positive and negative endpoints of the z-axis in $\mathbb{R}^3$ (which correspond to the positive and negative endpoints of the z-axis in $F_9 = 0$ and $F_{10} = 0$).

The possible ω-limits are the points Q_9 on $F_9 = 0$, and the equivalent in $F_{10} = 0$, which both correspond with the equilibrium point P_1 in $\mathbb{R}^3$; the positive endpoint of the x-axis in $F_9 = 0$ and the negative endpoint of the x-axis in $F_{10} = 0$, which correspond to the infinite points S_1 and S_2; and also the positive and negative endpoints of the z-axis, but only for the orbits over the infinity in $F_9 = 0$ and $F_{10} = 0$, which are the separatrices in the region with $y < 0$ in $\mathbb{R}^3$.

With a similar reasoning we can analyze the following cases.

If $\lambda > 0$ and $\kappa < 0$ the possible α-limits for any point $p \in \mathbb{R}^3$ are the infinite points S_3 and S_4, and also the positive and negative endpoints of the z-axis. The possible ω-limits are the infinite points S_1 and S_2, and also the positive and negative endpoints of the z-axis in the case of the four separatrices in the region with $y < 0$.

If $\lambda = 0$ and $\kappa > 0$ the possible α-limits for any point $p \in \mathbb{R}^3$ are the infinite points S_3 and S_4, the positive endpoints of the z-axis and also the negative endpoint of the z-axis in the case of the four separatrices in the region with $y > 0$ and $z > 0$. The possible ω-limits are the finite points over the straight line $(0, 1-\kappa, z)$ with $z \in \mathbb{R}$, the infinite points S_1, S_2, the positive endpoints of the z-axis, and also the negative endpoints of the z-axis in the case of the separatrices in the region with $y < 0$ and $z < 0$.

If $\lambda = 0$ and $\kappa < 0$ the possible α-limits for any point $p \in \mathbb{R}^3$ are the finite points over the straight line $(0, 1-\kappa, z)$ with $z \in \mathbb{R}$, the infinite points S_3, S_4, the positive endpoint of the z-axis, and also the negative endpoint of the z-axis for the separatrices in the region with $y > 0$ and $z < 0$. The possible ω-limits are the points S_1, S_2, the negative endpoints of the z-axis, and also the positive endpoints of the z-axis for the separatrices in the region with $y < 0$ and $z > 0$.

If $\lambda < 0$ and $\kappa > 1$ the possible α-limits for any point $p \in \mathbb{R}^3$ are the infinite points S_3 and S_4, and also the positive and negative endpoints of the z-axis in the case of the four separatrices in the region with $y > 0$. The possible ω-limits are the infinite points S_1, S_2, and the positive and negative endpoints of the z-axis.

If $\lambda < 0$ and $\kappa < 0$ the possible α-limits for any point $p \in \mathbb{R}^3$ are the finite point P_1 and the infinite points S_3 and S_4, also the positive and negative endpoints of the z-axis in the case of the four separatrices in the region with $y > 0$. The possible ω-limits are the points S_1, S_2, and the positive and negative endpoints of the z-axis.

Acknowledgements

The first and third authors are partially supported by the Ministerio de Ciencia e Innovación, Agencia Estatal de Investigación (Spain), Grant PID2020-115155GB-I00 and the Consellería de Educación,Universidade e Formación Profesional (Xunta de Galicia), Grant ED431C 2023/31 with FEDER funds. The second author is partially supported by the Agencia Estatal de Investigación of Spain grant PID2022-136613NB-100, and by the Reial Acadèmia de Ciències i Arts de Barcelona. The fourth authors is partially supported by FCT/Portugal through CAMGSD, IST-ID, projects UIDB/04459/2020 and UIDP/04459/2020.

References

[1] A. Cima, J. Llibre, Bounded polynomial vector fields, *Trans. Amer. Math. Soc.* **318**(1990) 557–579. https://doi.org/10.1090/S0002-9947-1990-0998352-5

[2] R. Devaney, Collision oribts in the anisotropic Kepler problem, *Inventiones Math.* **45**(1978) 221–251. https://doi.org/10.1007/BF01403170

[3] F. Dumortier, J. Llibre, J. C. Artés, *Qualitative theory of planar differential systems*, UniversiText, Springer-Verlag, New York, 2006. https://doi.org/10.1007/978-3-540-32902-2

[4] R. Hide, A. C. Skeldon, D. J. Acheson, A study of two novel self-exciting single-disc homopolar dynamos: theory, *Proc. R. Soc. London Ser. A* **452**(1996), 1369–1395. https://doi.org/10.1098/rspa.1996.0070

[5] H. W. Hirsch, C. C. Pugh, M. Shub, *Invariant manifolds*, Lecture Notes in Mathematics, Vol. 583, Springer-Verlag, Berlin, 1977.

[6] X. Li, New insights to the Hide–Skeldon–Acheson dynamo, *Discrete Contin. Dyn. Syst. Ser. B* **27**(2022), No. 11, 6257–6267. https://doi.org/10.3934/dcdsb.2021315

[7] J. Llibre, M. Messias, R. P. da Silva, On the global dynamics of the Rabinovich system, *J. Phys. A* **41**(2008), 275210, 21 pp. https://doi.org/10.1088/1751-8113/41/27/275210

[8] J. Llibre, R. Oliveira, Quadratic systems with an invariant conic having Darboux invariants, *Comm. Contem. Math.* **20**(2018), 1750033, 15 pp. https://doi.org/10.1142/S021919971750033X

[9] A. Mahdi, C. Valls, Integrability of the Hide–Skeldon–Acheson dynamo, *Bull. Sci. Math.* **138**(2014), 470–482. https://doi.org/10.1016/j.bulsci.2013.04.001